Saudi Pharmaceutical Journal 31 (2023) 101687

HOSTED BY

Contents lists available at ScienceDirect

Saudi Pharmaceutical Journal

journal homepage: www.sciencedirect.com

Original article

Isolation, characterization, development and evaluation of phytoconstituent based formulation for diabetic neuropathy

Rashmi Pathak [a], Neetu Sachan [b], Atul Kabra [c], Ashwag S. Alanazi [d], Mohammed M. Alanazi [e], Nawaf A. Alsaif [e], Phool Chandra [f,*]

[a] Department of Pharmacy, Invertis University, Bareilly-243123, Uttar Pradesh, India
[b] Maharana Pratap College of Pharmacy, Mandhana, Kanpur-209217, Uttar Pradesh, India
[c] University Institute of Pharma Sciences, Chandigarh University, Gharuan, 140301 Mohali, Punjab, India
[d] Department of Pharmaceutical Sciences, College of Pharmacy, Princess Nourah bint Abdulrahman University, P.O. Box 84428, Riyadh 11671, Saudi Arabia
[e] Department of Pharmaceutical Chemistry, College of Pharmacy, King Saud University, Riyadh [aadea], Saudi Arabia
[f] Teerthanker Mahaveer College of Pharmacy, Teerthanker Mahaveer University, Moradabad-244001, Uttar Pradesh, India

ARTICLE INFO

Article history:
Received 24 April 2023
Accepted 19 June 2023
Available online 24 June 2023

Keywords:
Morus alba
Isolation
Chrysin
Nanoemulsion
Diabetic Neuropathy

ABSTRACT

Background: *Morus alba* Linn, referred to as white mulberry, is a potential traditional medicine for diabetes and neuroprotection.
Aim: Isolation, characterization, development and evaluation of phytoconstituent based formulation for diabetic neuropathy.
Material and methods: The stem Bark of *M. alba* was peeled and subjected to extraction. A phytoconstituent was then isolated by column chromatography and characterized using Mass spectroscopy, FTIR, and NMR. The isolated phytoconstituent was used to formulate a nanoemulsion. Nanoemulsion was also characterized for viscosity, surface tension, refractive index, pH, and particle size. Selected nanoemulsion formulations were then tested for acute oral toxicity and diabetic neuropathy, including behavioral, hematological, histopathological, and biomarker examinations.
Results: The spectral analysis affirmed that the isolated compound was found to be chrysin. A nanoemulsion formulation was made using the chrysin and was characterized and found to be stable during the stability testing and fulfilled all other testing parameters. Then acute oral toxicity study of the formulations was found to be safe. Formulations were found to possess significant results against diabetic neuropathy in rats. Biomarkers were analyzed for their mechanistic involvement in reducing neuropathy in rats, and it was found that the oxidative pathway was considerably restored, suggesting that chrysin causes these effects via this pathway.
Conclusions: Results suggests that isolated phytoconstituent (chrysin) from the bark of *Morus alba* derived nanoemulsion has protective and beneficial effects by diminishing the oxidative damage against alloxan-induced diabetic neuropathy in rats.

1. Introduction

Neuropathy is the degeneration of nerves that begins from the toes and can extend to other body parts (Callaghan et al., 2012). It is divided based on the area of the brain where neurons are most damaged: autonomic, focal, proximal, and peripheral, with each group exhibiting a variety of disorders like stomach problems, numbness, and cardiac problems (Grover et al., 2020). Diabetes has many negative effects, including diabetic neuropathy, which is the main factor in excruciating nerve injury. Diabetic neuropathy is caused by variations in the blood vessels that supply the

* Corresponding author.
E-mail addresses: rashmipathak963@gmail.com (R. Pathak), profneetusachan@gmail.com (N. Sachan), atul.kbr@gmail.com (A. Kabra), asalanzi@pnu.edu.sa (A.S. Alanazi), mmalanazi@ksu.edu.sa (M.M. Alanazi), nalsaif@ksu.edu.sa (N.A. Alsaif), profpcpatel@gmail.com (P. Chandra).

Peer review under responsibility of King Saud University. Production and hosting by Elsevier.

Production and hosting by Elsevier

https://doi.org/10.1016/j.jsps.2023.06.020
1319-0164/

peripheral neurons, metabolic issues such as enhanced myo-inositol depletion, stimulant of the polyol pathway, and enhanced non-enzymatic glycation (Zychowska et al., 2013, Pathak et al., 2022).

Globally, more than 40 million people with diabetes live with neuropathy (Baxi et al., 2020). Along with diabetic nephropathy, diabetic cardiomyopathy, and diabetic retinopathy, diabetic neuropathy, is one of the most serious health effects of diabetes. About 20% of persons with diabetes get, a painful and serious consequence of the condition. Diabetes-related nerve degeneration leads to diabetic neuropathy. Diabetes results in high levels of triglycerides, a type of blood fat, and excessive blood glucose, which, over time, can affect your nerves. Depending on the type, diabetic neuropathy manifests differently. The symptoms of this condition can range from numbness and soreness in the feet to problems with the heart and bladder. Diabetes patients who exhibit symptoms and evidence of peripheral nerve damage after other potential causes have been ruled out are said to have diabetic neuropathy. Based on the locations of the most impacted neurons, it is categorized into autonomic, peripheral, proximal, and focal (Zychowska et al., 2013, Pathak et al., 2022).

Mulberry (*Morus alba* L.) belongs to the Moraceae family's Morus genus (Ercisli and Orhan 2007). Ramulus Mori or Sangzhi are other names for mulberry (Ye et al., 2002). This genus has been documented to have 24 species and 100 variants (Ercisli and Orhan 2007). These are found largely in temperate regions, with some expanding into African tropical areas and the Andes in South America. In China, there are 11 different species. One such example is the genus Morus (mulberry), which has approximately 150 species, the most prevalent of which is *M. alba* L (Srivastava et al., 2006). Typically, it is feed as leaves to ruminants and *Bombyx mori* L. (silkworms). *M. alba* and other Mulberries are produced in several countries, including Turkey and Greece, to produce fruit that has a specific application in various traditional meals (Arabshahi-Delouee and Urooj 2007). Different parts of *Morus alba* were found to posses the antidiabetic potential (Zhang et al., 2022, Batiha et al., 2023). Aqueous mulberry (*Morus alba* L.) fruit extract was employed in a biofunctional reducing agent for the environmentally friendly synthesis of copper (Cu), palladium (Pd) and silver (Ag), metallic nanoparticles (NPs) and resulted in antibacterial efficacy against *Escherichia coli* O_{157}:H_7 and *Listeria monocytogenes* (Razavi et al., 2019). In a study, the antibacterial and neoplastic potential of silver nanoparticles (AgNPs) made from *Morus alba* leaf extract (MLE) was evaluated. The presence of phenolic chemicals that act as reducing, capping, and stabilizing agents in the biosynthesis of AgNPs was validated by the GC–MS analysis of MLE. The findings validate the significant antibacterial and anticarcinogenic potential of white mulberry leaf extract-produced AgNPs (Kumkoon et al., 2023). On the basis of literature, we planned to isolate, characterize phytoconstituent and then develop and evaluate phytoconstituent based formulation for diabetic neuropathy.

2. Materials and methods

2.1. Identification, collection and plant material authentication

In January, *Morus alba* stem bark samples were collected at the IFTM University's Botanical Garden in Moradabad, India (28°52′54.2″N 78°43′23.2″E). The bark was washed and air-dried. Authentication was done by the Chief Scientist, RHMD, CSIR-NIScPR, Delhi, India. A voucher specimen (Authentication No.: NIScPR/RHMD/Consult/2022/4031–32) was submitted to the department for further use.

2.2. Drugs and chemicals

Procurement of chemicals was done from Central Drug House Ltd., New Delhi, India and Metformin as the standard drug (purity: 99.9%) was available from CDH (P) Ltd., Delhi, India.

2.3. Macroscopical evaluation of Morus alba's bark

The term ''macroscopical evaluation" refers to the assessment of pharmaceuticals based on their colour, odour, taste, form, and specific characteristics such as touch and texture. It's a method of assessing quality based on the analysis of morphological profiles of the bark (Nagani et al., 2012, Onyambu et al., 2020).

2.4. Extraction

The stem bark was gathered, washed under running water, and dried outside for two to three weeks. The yellowish layer underlying was revealed by lightly scraping the completely dry stem. The stem bark or cortex was removed with a knife, cut into small pieces, and powdered in a blender. A fine, uniform powder was created by sieving the raw powder. For ten days, *M. alba* stem bark powder was steeped in 75% ethanol, then shaken. Filtering was done on the extract. The residue was extracted once more with fresh ethanol to ensure thorough extraction. For testing, the filtrates were sieved, air-dried to a powder, and maintained at 4°C (Rauf et al., 2015).

2.5. Phytochemical screening

The extract obtained was exposed to various chemical tests to determine their phytoconstituents (Trease and Evans 1983, Sofowora 1996).

2.6. Isolation

The extract was exposed to column chromatography on a silica gel (Merck Silica gel 60/0.063–0.200 mm). The column was filled using a solvent solution of n-hexane: ethyl acetate (3:7). There were three sub-fractions identified: A, B, and C. Isolated compound with an estimated Rf value of 0.76, was isolated from sub-fraction B (n-hexane–ethyl acetate; 3:7). Then it was concentrated, and 99 mg was collected. The extraction method mentioned above has been repeated numerous times to procure enough isolated compound for the tests. Characterization was completed using NMR, FTIR, and mass spectroscopy.

2.7. Development of oil-in-water nanoemulsions

The formulations in Table 1 were used to make Phytoconstituent-loaded oil-in-water Nanoemulsion. The oil phase was composed of sorbitan monooleate (Span 80; 1–2.5% w/w), ethanol (7.5% w/w), and Coconut oil (7.5% w/w). Water (80–83%) and polysorbate 20 (Tween 20; 1–2.5% w/w) make up the water phase. The water and oil phases were heated to 60°Celsius while swirling to create an emulsion. For three minutes, the two phases were blended and homogenized at a speed of 10,000 rpm. Finally, the chrysin-Nanoemulsion was developed by passing the pre-emulsion through a microfluidizer (Microfluidizer, Canada). Next, we looked at the particle size distribution, average particle size, and surface charge of phytoconstituent-NE nano colloids (Ting et al., 2021).

Table 1
oil and water phase compositions in the prepared Oil-in-water nanoemulsions.

Formulation	Oil Phase (% w/w)			Water Phase (% w/w)	
	Coconut oil	Ethanol[a]	Sorbitan monooleate	polysorbate 20	Water
F1	7.5	7.5	2.5	2.5	80
F2	7.5	7.5	2	2	81
F3	7.5	7.5	1.5	1.5	82
F4	7.5	7.5	1	1	83

[a] Containing 2.5 mg/mL chrysin.

2.8. Characterization of nanoemulsion

2.8.1. Physical parameters

Physical parameters of developed nanoemulsions were determined, such as colour, odour, and storage condition.

2.8.2. Measurement of pH

A (30 ml) sample was placed in beakers with a capacity of (50 ml) to determine the pH of all generated NEs using a pH meter device (Ali and Hussein 2017). All measurements were repeated three times.

2.8.3. Determination of refractive index

By employing a drop of the formulation on the slide and comparing it to the refractive index of water, i.e., 1.333, the Abbes refractometer at 25 ± 0.5° was used to measure the nanoemulsion's refractive index. If a nanoemulsion's refractive index is equal to the refractive index of water, the nanoemulsion is considered transparent (Baboota et al., 2007, Liang et al., 2021).

2.8.4. Determination of viscosity

The viscosity measurement is a significant factor in the physicochemical characterization of nanoemulsions. An viscometer was used to determine a nanoemulsion's viscosity (Baboota et al., 2007, Liang et al., 2021).

2.8.5. Determination of surface tension

A stalagmometer was used to measure surface tension using the drop count method (Gupta and Kompella 2006).

2.8.6. Determination of Zeta potential

The Malvern Zeta sizer instrument was used to measure it. Zeta potential, which was computed based on the electrophoretic mobility of oil droplets, was measured by diluting Nanoemulsion (Dordevic et al., 2017).

2.8.7. FESEM examination

The image was created step-by-step by scanning a focused electron beam across the material when using the FESEM JSM 6100 for assessment. Numerous elastic scattering processes diverted the source electrons after they had pierced the solid material. The effect of the incident electrons caused a variety of signals to be produced, which were then gathered to create an image or examine the sample surface (Bogner et al., 2007, Brodusch et al., 2018).

2.8.8. Stability study

The ideal nanoemulsion formulations were stored at −18 °C in the refrigerator for three months and 75% relative humidity (RH) and 40 °C in an oven to test their physical stability. Zeta potential, refractive index, viscosity, pH, and surface tension are among the NE properties after one and three months of storage (Yadav et al., 2014).

2.9. Experimental animals

Wistar rats, either sex, of weight 150 to 250 g, were procured from the IFTM University's animal house. The animals (n = 36) were housed in polypropylene cages at 28 °C, 60–70% relative humidity, and a 12:12 h light/dark cycle. The animal had full access to standard pellet feed during the experiment. Mineral water was readily accessible to the animal. The Institutional Animal Ethics Committee at IFTM University in Moradabad approved the pharmacology and acute toxicity protocols with reference number no. CPCSEA 837/PO/ReBiBt/S/04/CPCSEA/9.

2.10. Acute oral toxicity studies

Acute oral toxicity is the term used to describe the adverse effects that follow the administration of a single dosage of a substance or many doses within a 24-hour period. According to the recommendations of guideline 423 of the Organization for Economic Cooperation and Development (OECD), the greatest feasible dose of 2000 mg/kg will be applied. For the test, three rats were used, each dosed at a 48-hour interval. Skin, fur, mucus membrane (nasal), eyes, autonomic salivation, urine, sweat, piloerection, lacrimation, incontinence, and feces) and CNS (drowsiness, gait, tremors, and convulsion) alterations are observed once daily in the cage. Over two weeks and mortality will be identified (OECD 2002). Histopathological and Hematological parameters were also estimated (Slaoui and Fiette 2011).

2.11. Induction of diabetes to the animals by alloxan-induced diabetes model

To validate the efficiency of Nanoemulsion formulation in experimental diabetic conditions, to induce pharmaceutical diabetes, alloxan monohydrate (Central Drug House Ltd., New Delhi) was utilized. A 150 mg/kg intraperitoneal injection of Alloxan monohydrate was dissolved in cold normal saline (0.9% w/v) to induce diabetes in male Wistar rats that had been starved overnight (12 h). To prevent hypoglycemia, the rats were kept in their cages for the next 24 h, and 10 % glucose solution was maintained by providing them in bottles. The fasting blood glucose level was tested 72 h after the injection. Animals that did not reach glucose levels of 200 mg/dL or above were not included in the study. During the trial, fasting blood glucose was assessed using a glucometer (Banda et al., 2018).

2.12. Treatment schedule and experimental protocol

Thirty Wistar rats were used for the investigation, of which six were part of the normal control group. The remaining animals were all given diabetes through induction. Animals in group 1-the normal Control Group, received distilled water and were kept diabetic-free. Diabetes control, group 2 treated with alloxan received oral saline. In Group 3, F2 was used to treat hyperglycemia brought on by alloxan. In Group 4, F3 was used to treat

hyperglycemia brought on by alloxan. In Group 5, metformin (500 mg/kg/day) was the standard of care for alloxan-induced diabetes. The medications were given orally for eight weeks in a row and blood glucose level was measured. Table 2 shows the grouping of animals for the alloxan-induced diabetic neuropathy model study (Valcheva-Kuzmanova et al., 2015).

2.13. Development of diabetic neuropathy

To assess the effects of diabetic neuropathy, the medication was continued from week 0 to week 8. Tail immersion test, Eddy's hot plate method, Actophotometer, and Rotarod tests were used to accurately assess the progression of diabetic neuropathy in each group on the second, fourth, and eighth weeks of the study, respectively.

2.14. Observation of physical parameters of hyperglycemic rats

Eyes, fur, skin, mucous membrane, lacrimation, incontinence, perspiration, salivation, piloerection, urinary, and defecation were observed during the study.

2.15. Measurement of blood glucose level

A test strip was placed inside a glucometer. inserted a lancet into the glucometer's included lancing device. The blood flow was enabled when the lancing tool's tip was gently placed against the skin's surface close to the exposed tail tip. A tiny blood droplet was visible on the skin's surface. A blood drop was placed on the sample end (active region) of the glucometer test strip. waited for the blood sample to be processed by a glucometer (about 5 s), then recorded the plasma glucose level in mg per dl (Morrow 2004).

2.16. Behavioral test

2.16.1. Assessment of thermal hyperalgesia

The variations in pain threshold values were evaluated in the normal control, diabetic control, standard, test 1 and test 2 groups of rats in the second, fourth, and eighth weeks following a basal observation of nociceptive thresholds of post-alloxan injection. Using Eddy's hot plate method for determining sensitivity to unpleasant thermal stimuli, thermal hyperalgesia of the hind paw was examined (Eddy et al., 1950). In addition, the tail immersion test was used to determine spinal temperature sensitivity (Necker and Hellon 1978).

2.16.1.1. Tail-Immersion (Hot Water/Heat-Allodynia) test. The tip of the rat's tail (1 cm) was placed in a hot water bath kept at 52.5 ± 0.5 °C and left there until the tail removal delay (flicking reaction) or signs of struggle manifested themselves (cut-off 20 s). A decrease in tail withdrawal time is a sign of hyperalgesia (Kanaan et al., 1996).

2.16.1.2. Hot-Plate (Heat-Allodynia) test. A mix of central and peripheral processes is assumed to be responsible for the hot-plate hyperalgesic response. The rats were set on top of an Eddy's hot plate that had been preheated and maintained at a constant temperature of 55 ± 1 °C. The amount of time it took for the initial sign of paw licking or a leaping reaction to escape the heat was used to determine the pain threshold. The cut-off time was set to 20 s to prevent paw harm (Kanaan et al., 1996, Saraswat et al., 2020a, 2020b).

2.16.2. Motor coordination (Rotarod test)

Animals from each group were placed on a rod that was revolving at a speed of 20–25 rpm as soon as the device was turned on. Only the rats that showed the capacity to stay on the rotating rod (20–25 rpm) for five minutes after training sessions were chosen for the tests. Each group kept a record of the fall-off time. A decrease in fall-off time is indicative of central nervous system depression (CNS) (Deacon 2013).

2.16.3. Locomotor activity (Actophotometer Test)

Rat locomotor activity was observed using an Actophotometer to gauge the CNS depressant action. There were five groups created from the rats. Rats from each group were placed separately in the activity cage for 5 min while the apparatus was turned on. The basal activity score for each animal was then tracked and recorded (Kulkarni 2005). Percent reduction in motor activity was calculated.

2.17. Biochemical estimations from sciatic nerve homogenate

The sciatic nerves were separated from the rats when they were slaughtered at the conclusion of the 8-week research. Then, a tissue homogenate was created by a buffer containing Tris-HCl 0.1 M at a 7.4 pH, and the homogenate's supernatant was utilized to calculate the amounts of SOD (superoxide dismutase), Na^+K^+-ATPase, NO content (nitric oxide), lipid peroxidation (MDA content-LPO), and TNF-α (Bonting 1970, Sriraksa et al., 2019).

2.18. Histopathological examination

Under light Ketamine anesthesia, the rats' sciatic nerve, livers, stomach and kidneys were removed and rinsed in normal saline; small bits of tissue were collected in 10% formalin solution. Histopathological examinations of organs were done and observed the changes (Slaoui and Fiette 2011).

2.19. Statistical analysis

The findings were shown as mean ± SEM. The statistical analysis of all the gathered data was accomplished using a one-way analysis of variance (ANOVA: Dunnett's test). The changes were considered significant at $p < 0.05$. The software Graph Pad Prism 5 was used to conduct the statistical analysis.

Table 2
Alloxan-induced diabetes model for diabetic neuropathy.

S. No	Group	Drug	Dose (mg/kg)	Animals
1	Normal control	Distilled water		6
2	Diabetic control	Normal Saline Solution		6
3	Test 1	F2	10	6
4	Test 2	F3	10	6
5	Standard	Metformin	500	6

3. Results

3.1. Macroscopical evaluation of Morus alba's bark

Table 3 shows some macroscopical characteristics of bark of *Morus alba* and Fig. 1 shows picture of bark.

3.2. Percentage (%) Yield of extract

Percentage (%) Yield = 7%w/w.

3.3. Preliminary phytochemical screening

Phytochemical analysis of an ethanolic extract of *Morus alba* (EEMA) discovered alkaloids, tannins, saponins, flavonoids, anthraquinone glycosides, carbohydrates and proteins were present in the extract, whereas monosaccharide and amino acids were found to be absent in the extract. The results of the phytochemical screening are shown in Table 4.

(-) negative, (+) Positive.

3.4. Column chromatography

The extract was exposed to column chromatography on a silica gel (Merck Silica gel 60/0.063–0.200 mm). The column was filled using a solvent solution of n-hexane: ethyl acetate (3:7). There were three sub-fractions identified: A, B, and C. A distinct compound, with an estimated Rf value of 0.76, was isolated from sub-fraction B (n-hexane–ethyl acetate; 3:7). Then it was concentrated using rotary evaporator (Buchi Rotavapor, New Castle, DE) and 99 mg was collected. To acquire enough isolated compound for the tests, the extraction method mentioned above was repeated numerous times. Characterization was completed using NMR, FTIR, and mass spectroscopy.

3.5. Characterization of an isolated compound

The yellow solid, isolated compound made from fraction B of ethyl acetate extract. A Compound was discovered to have a melting point between 282 °C and 285 °C. The functional groups or chemical entities found in isolated compound were revealed by the FTIR spectra. The compound's structure was determined based on FTIR, Mass spectroscopy, and NMR spectra, and it was well in line with the structure of chrysin.

Table 3
Macroscopical characteristic of *Morus alba*'s bark.

Property	Result
Colour	Greyish Brown
Odour	Odourless
Taste	Sweet
Shape	Flat
Texture	Rough shining

Table 4
Preliminary phytochemical components found in the bark of EEMA.

S. No.	Chemical Test	Result of EEMA
1	Saponins	+
2	Tannins	+
3	Alkaloids	+
4	Proteins	+
5	Anthraquinone glycosides	+
6	Monosaccharide	–
7	Carbohydrates	+
8	Flavonoids	+
9	Amino acids	–

(-) negative, (+) Positive.

3.5.1. Fourier transform infrared spectroscopy

Different peaks in FTIR spectra of isolated compound were shown in Fig. 2. IR (KBr) Vmax: 3065.98 cm^{-1} (O—H Stretching); 2967.61 cm^{-1} (C—H stretching); 1648.24 cm^{-1} (C=O Stretching); 1613.52 cm^{-1} (C=C); 1356.98 cm^{-1} (C—O stretching); 1459.21 cm^{-1} (C—O—H stretching); 1356.98 cm^{-1} (C—O—C stretching); 807.24 cm^{-1} (O—H stretching).

3.5.2. Nuclear magnetic resonance spectroscopy

1H NMR and 13C NMR of the isolated compound is shown in Fig. 3 and Fig. 4, respectively.

^{1}H NMR (DMSO d_6, δ ppm, 500 MHz): 7.77 (C–H); 6.71 (H); 6.02 (CH); 7.77 (CH); 7.48 (CH); 7.46 (CH); 6.71 (H).

^{13}C NMR (δ ppm, 500 MHz, DMSO-D6): C1-163.6, C2-158.8, C3-182.1, C4-161.8, C4-166.4, C5- 104.4, C6-130.3, CH1-104.5, CH2-94, CH3– 98.3, CH4- 127.9, CH5- 127.9, CH6- 127.9, CH7-128.6, CH8-128.6, CH9-127.9.

3.5.3. Mass spectroscopy

Mass spectroscopy as shown in Fig. 5 of isolated compound has the molecular formula $C_{15}H_{10}O_4$ based on ES-MS (FAB) $[M + 1]^+$ (m/z) and calculated molecular weight is 254.24 g/mol.

On the basis of structure elucidation using IR, ^{1}HNMR, ^{13}C NMR and Mass spectroscopy, the isolated compound was found as Chrysin (Fig. 6).

3.6. Characterization of formulation

3.6.1. Physical parameters

Different parameters were used for the assessment of the formulations, such as physical parameters shown in Table 5, measurement of pH and refractive index, viscosity, and surface tension are shown in Table 6 respectively.

Fig. 1. Stem Bark of *Morus alba*.

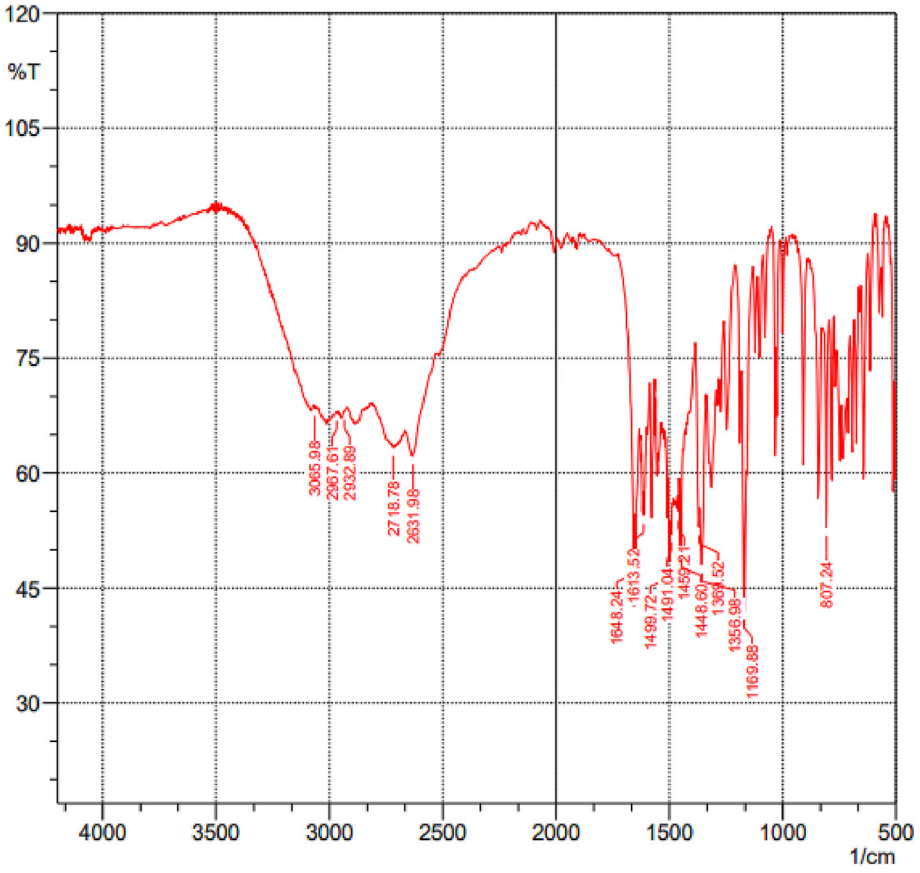

Fig. 2. FTIR spectra of isolated compound.

3.6.2. Measurement of pH and refractive index

The pH and Refractive index, Viscosity and surface tension of formulations are presented in the Table 6.

3.6.3. Stability testing

Stability testing was done for Nanoemulsion formulations as shown in Table 7. F2 and F3 passed the stability test and

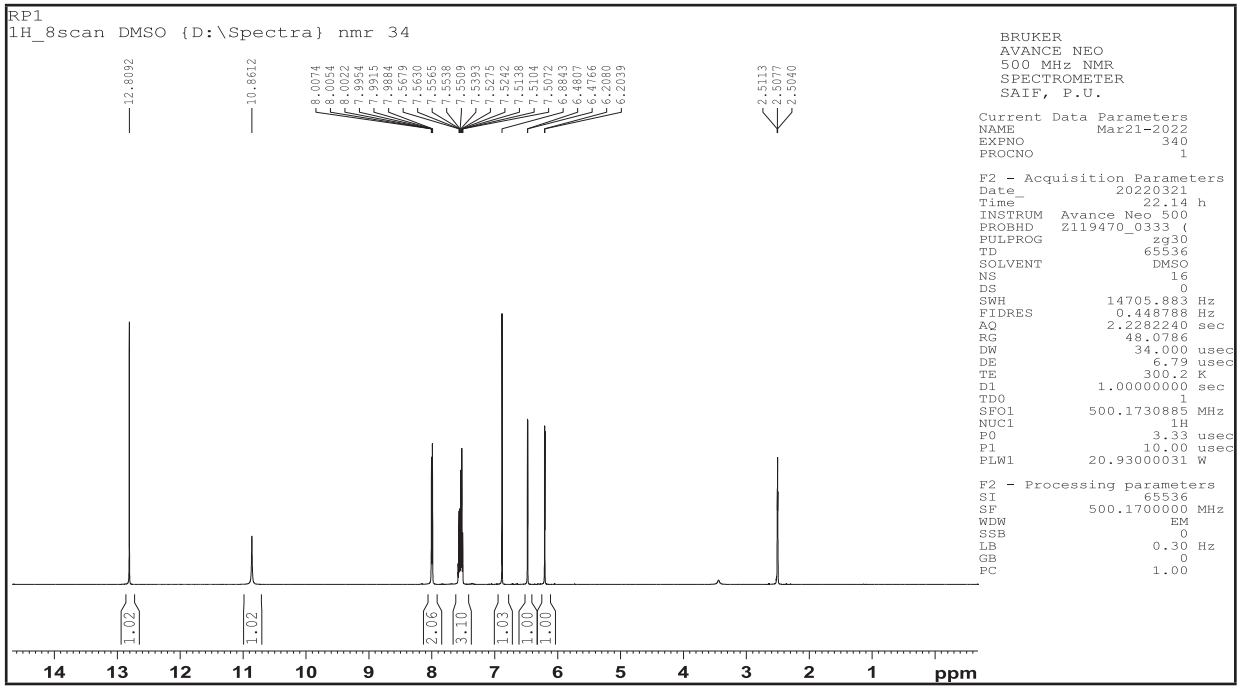

Fig. 3. ^{1}H NMR of isolated compound.

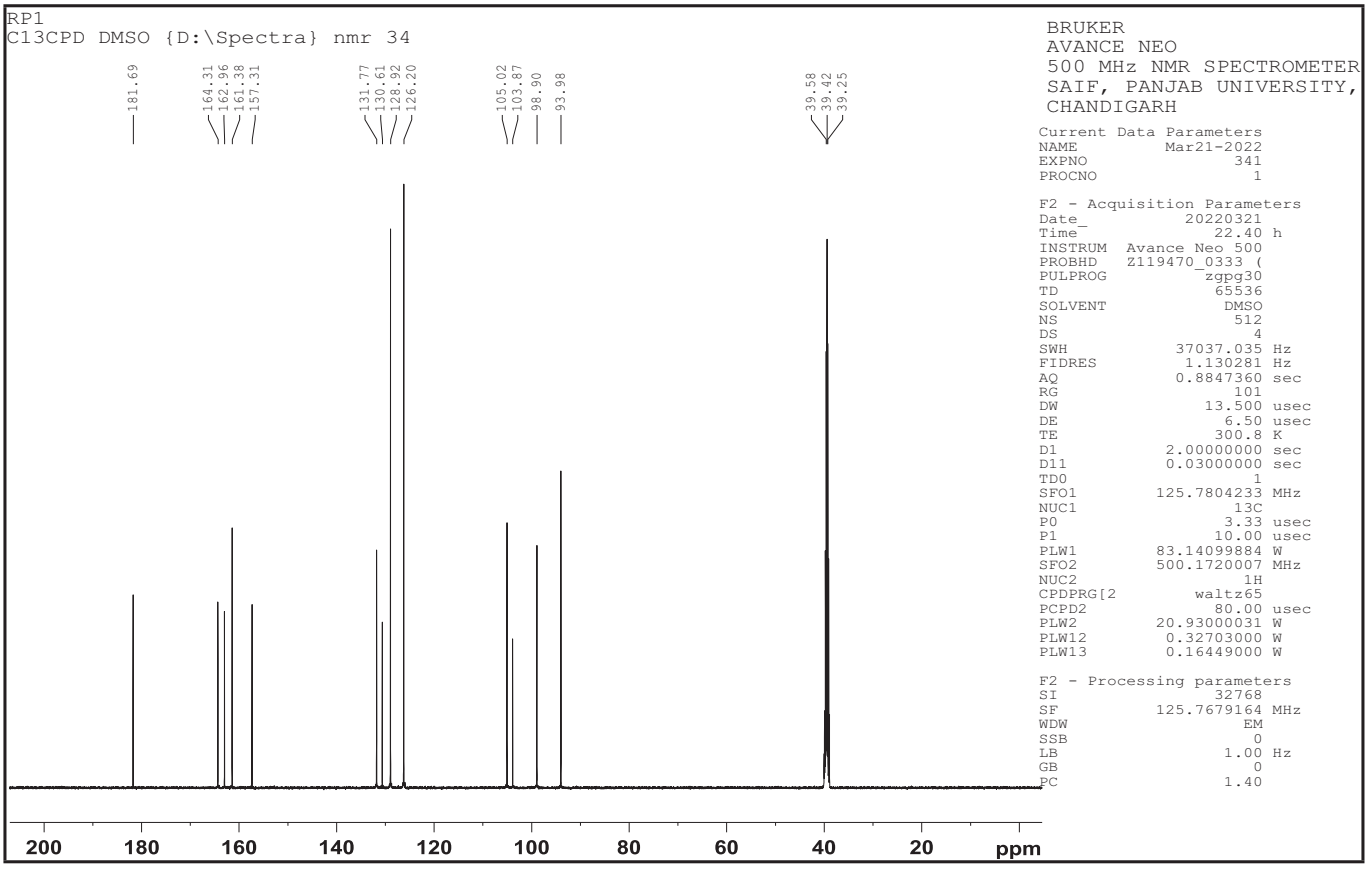

Fig. 4. ^{13}C NMR of isolated compound.

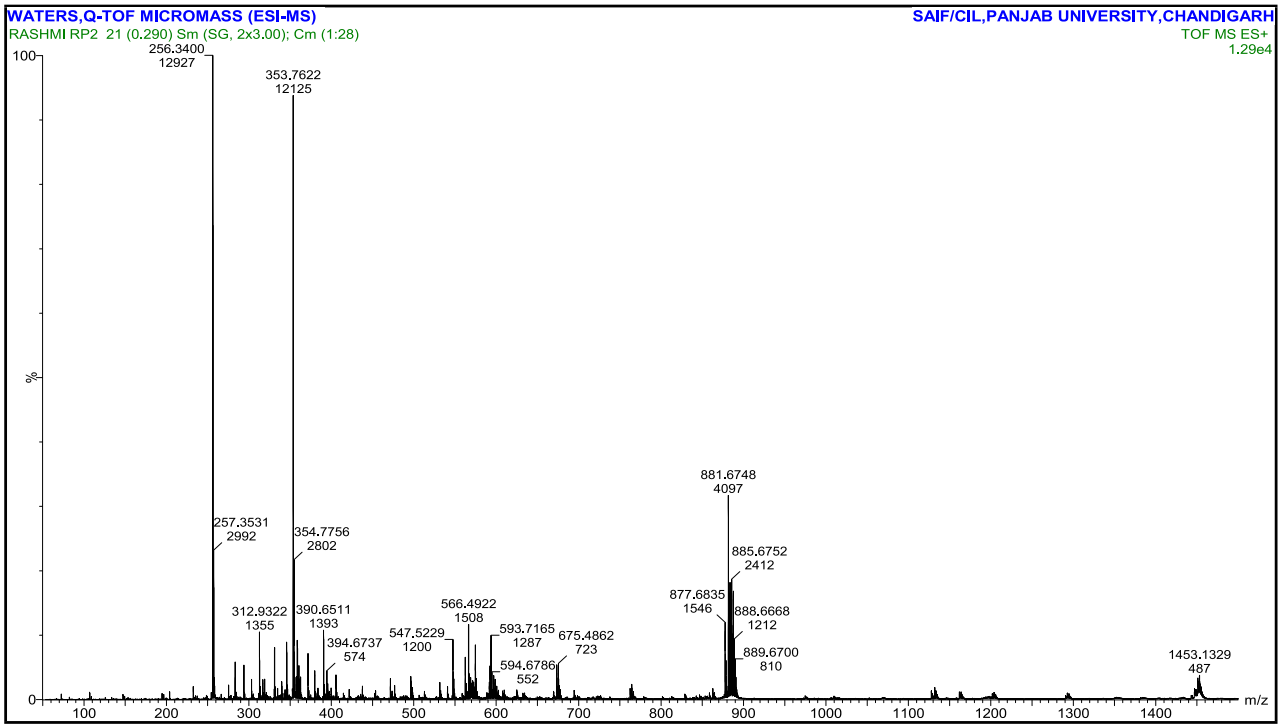

Fig. 5. Mass spectroscopy of isolated compound.

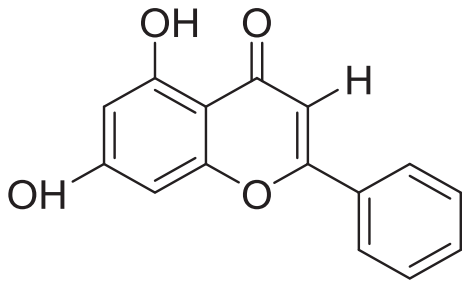

Fig. 6. Structure of Chrysin.

Formulation 1 and Formulation 4 showed the phase separation at 40 °C. So, F2 and F3 were used for further experimental work.

3.6.4. Zeta potential

The Zeta potential of F2 and F3 were found to be −10 mV and −8 mV, respectively (Fig. 7 and Fig. 8).

3.6.5. Determination of particle size

The formulations prepared were found to be in a range of 261.9 nm to 597.6 nm with F2 Avg 344.52 nm (PDI: 0.877) and F3 Avg 597.6 nm, (PDI:0.953), particle size analysis is shown in Fig. 9 and Fig. 10.

Table 5
Physical parameters of formulations.

Physical Parameters	F1	F2	F3	F4
Colour	Creamy white	Creamy yellow	Creamy yellow	Creamy yellow
Odour	Sweet	Sweet	Sweet	Sweet
Taste	Tasteless	Tasteless	Tasteless	Tasteless
Storage	25 °C	25 °C	25 °C	25 °C

Table 6
pH and Refractive index, Viscosity and surface tension of formulations.

Formulation	pH	Refractive index	Viscosity (Cp)	Surface tension (Dyne/cm)
F1	6.8	1.55	1.47	26.13
F2	7.1	1.54	1.34	26.98
F3	7.2	1.55	1.17	28.4
F4	6.9	1.56	1.08	30.6

Table 7
Stability Testing for Formulations.

Days	Freeze-thaw cycle freezing at (-18 °C for 20 h.)	Observation				Thaw cycle to the oven at (40 °C for 2 h)	Observation			
		F1	F2	F3	F4		F1	F2	F3	F4
1	After 20 **h**	N C	N C	N C	N C	After 2 **h**	N C	N C	N C	N C
2	After 20 **h**	N C	N C	N C	N C	After 2 **h**	N C	N C	N C	N C
3	After 20 **h**	N C	N C	N C	N C	After 2 **h**	N C	N C	N C	N C
4	After 20 **h**	N C	N C	N C	N C	After 2 **h**	N C	N C	N C	N C
5	After 20 **h**	N C	N C	N C	N C	After 2 **h**	N C	N C	N C	N C
6	After 20 **h**	N C	N C	N C	N C	After 2 **h**	P S	N C	N C	P S
7	After 20 **h**	N C	N C	N C	N C	After 2 **h**	P S	N C	N C	P S

NO Changes: N C.
Phase separation: P S.

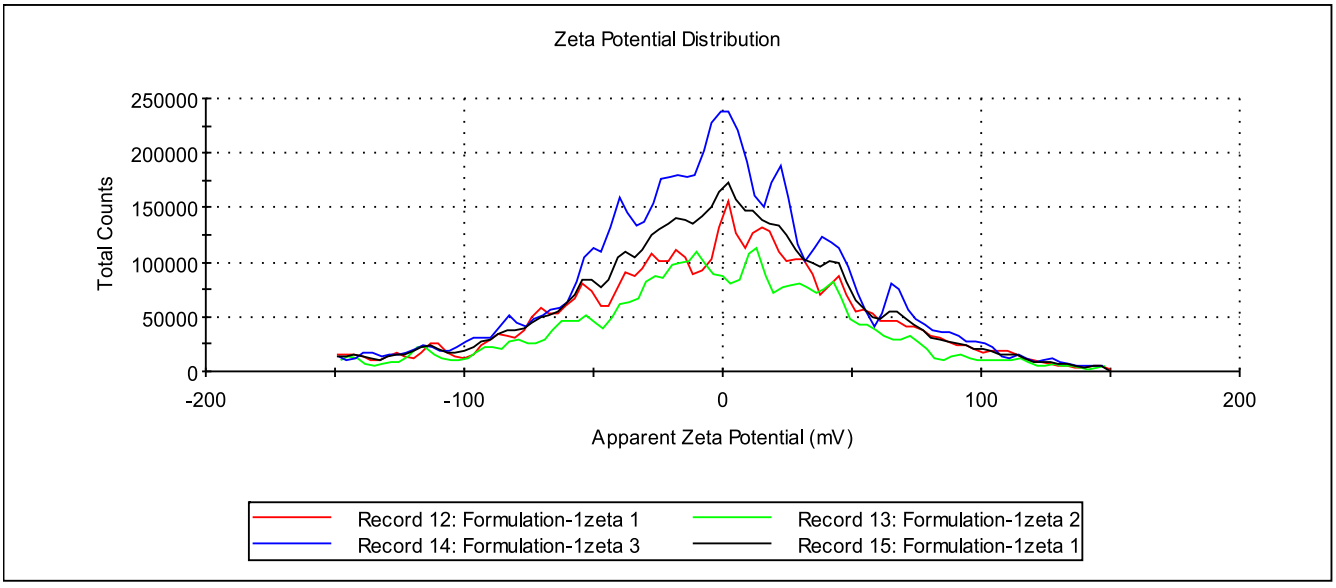

Fig. 7. Zeta potential distribution of F2.

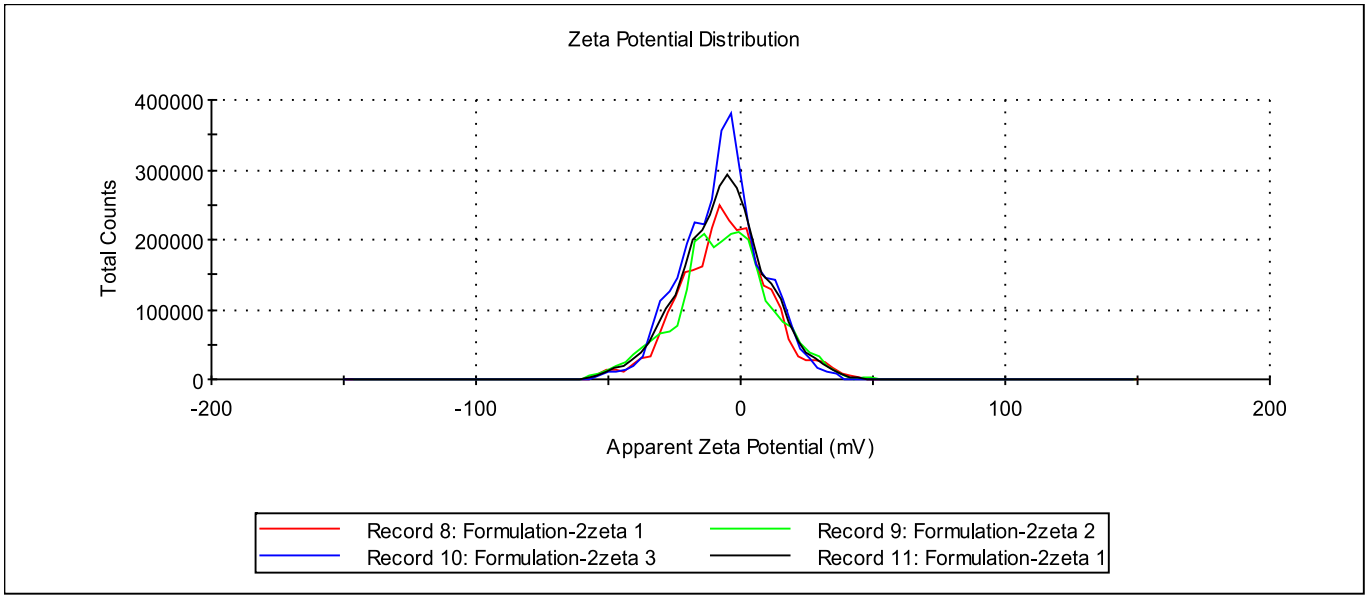

Fig. 8. Zeta potential distribution of F3.

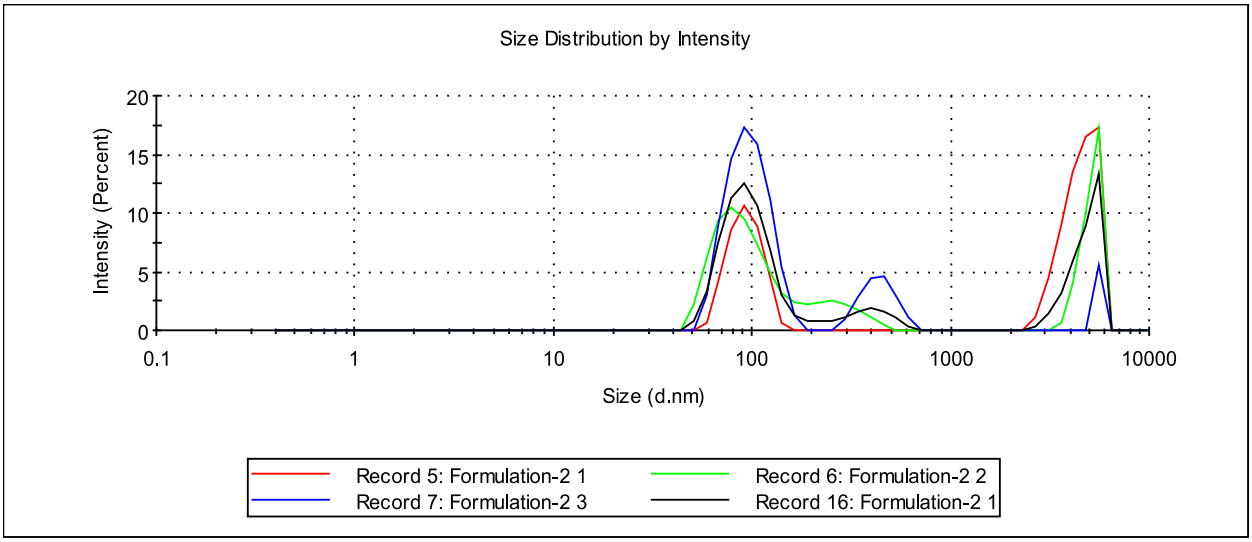

Fig. 9. Particle size distribution of F2.

3.6.6. Ftir spectroscopy

The results were obtained from the FTIR study of the spectrum of coconut oil as shown in Fig. 11A. The peaks between 3000 and 2800 cm^{-1} reflect the stretching vibration of the functional groups =C—H (alkene) and C—H (alkane), which were provided by the samples' esters chain. The presence of C=O stretching is evidenced by the distinctive peak in the coconut oil spectrum at a wavenumber of 1740 cm^{-1}. FTIR spectra of span 80 shows peaks at 2929 cm^{-1} (C—H stretching), 3574 cm^{-1} (O—H stretching), 1741 cm^{-1} (C=O stretching), 1175 cm^{-1} (C—O stretching) as shown in Fig. 11B. FTIR spectra of tween 20 shows peaks at 3737 cm^{-1} (O—H stretching), 2924 cm^{-1} (C—H stretching), 1817 cm^{-1} (C=O stretching), 1124 cm^{-1} (C—O—C stretching) as shown in Fig. 11C. FTIR spectra of F2 shows peaks at 3120 cm^{-1} (O—H stretching), 2854 cm^{-1} (C—H stretching), 1741 cm^{-1} (C=O stretching), as shown in Fig. 11D. FTIR spectra of F3 shows peaks at 3139 cm^{-1} (O—H stretching), 2855 cm^{-1} (C—H stretching), 1747 cm^{-1} (CO s=tretcing), as shown in Fig. 11E.

3.6.7. Field emission scanning electron microscopy (FESEM)

Optimized Nanoemulsion (O/W) was observed under FESEM (Fig. 12). In accordance with the particle size finding, Fig. 12 (A1) and Fig. 12(B1) shows minor discrete spherical particles with great homogeneity, and no significant clusters were detected. This showed that the O/W Nanoemulsion formulations had been effectively produced homogeneously and with a high degree of uniformity under the optimum emulsifier concentration and processing conditions found in this investigation.

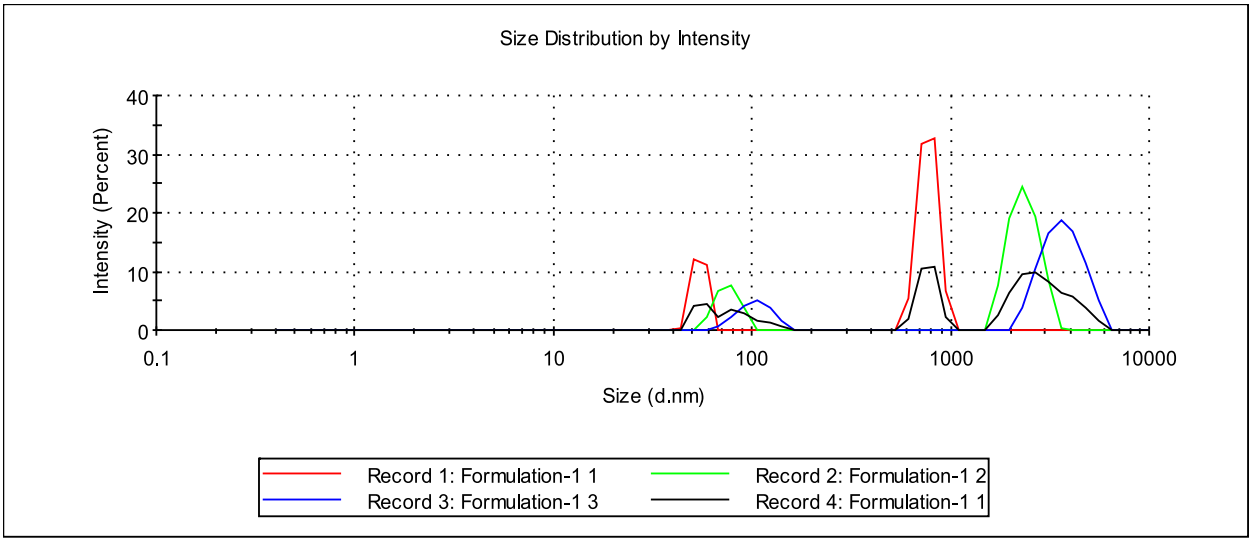

Fig. 10. Particle size distribution of F3.

3.7. Acute oral toxicity study

In the current study, both formulations were utilized for the acute oral toxicity study at 2000 mg/kg. Formulations were not found any type of toxicity in the treated animals. Therefore, two formulations were used for further study as shown in Table 8.

3.7.1. Evaluation of acute oral toxicity

The effect formulation during acute oral toxicity is presented in the Table 8.

3.7.2. Hematology for acute oral toxicity studies

Hematological parameters for the study of acute oral toxicity were assessed for the formulations, as shown in Table 9.

3.7.3. Histopathology

Histopathology of different organs such as liver, kidney, sciatic nerve, stomach, testis of rats was observed under microscopes for the changes as shown in Fig. 13. Liver demonstrating normal hepatocytes in both treated wirh F1 and F2. The renal tissue shows fairly well-preserved renal parenchyma. The renal tubules around renal corpuscles appeared apparently normal. Inflammatory changes in the renal parenchyma are not evident in F1 and F2 treated rats. F1 and F2 treated rats showed the normal arrangement of fibers. Also, normal histological structure of gastric mucosa were present. Formulations treated groups of rats showed appropriate testicular histology. The active seminiferous tubules and interstitial spaces demonstrating active spermatogenesis.

3.8. Evaluation of pharmacological parameters

3.8.1. Observation of physical parameters of hyperglycemic rats

Different physical parameters were observed during pharmacological study as shown in Table 10.

3.8.2. Assessment of body weight

Changes in body weight of rats were observed during the study as shown in Table 11.

3.9. Behavioral test

Behavioral assessment of rats was done during the study such as thermal hyperalgesia as shown in Table 12 and Table 13, motor coordination as shown in Table 14 and locomotor activity as shown in Table 15.

3.9.1. Evaluation of thermal hyperalgesia

3.9.1.1. Tail-Immersion (Hot Water/Heat-Allodynia) test. Results of F2 and F3 during evaluation of tail immersion test is presented in Table 12.

Values are demonstrated as Mean ± SEM; n = 6. One-way ANOVA; followed by Dunnett's test: $^{a}P < 0.05$ in comparison with normal control; $^{*}P < 0.05$, $^{**}P < 0.01$ and $^{***}P < 0.001$ in comparison with the diabetic control.

3.9.1.2. Hot-Plate (Heat-Allodynia) test. Results of F2 and F3 during evaluation of hot plate test is presented in Table 13.

3.9.2. Motor coordination (Rotarod Test)

Results of F2 and F3 during actophotometer test is presented in Table 14.

3.9.3. Locomotor activity (Actophotometer test)

Results of F2 and F3 during actophotometer test is presented in Table 15.

3.10. Biochemical estimations

3.10.1. Effect on superoxide dismutase

Comparatively to the normal group of rats (26.13 ± 1.75 μ/mg of protein), the amount of superoxide dismutase in the sciatic nerve of diabetic control group rats was significantly lower protein 5.51 ± 1.34 μ/mg. Whereas, in Group III and IV, respectively, the treated group rats showed an enhance in superoxide dismutase levels of protein (20.35 ± 1.34 μ/mg) and 24.28 ± 1.42 μ/mg. This has produced notable and dose-dependent effects in rats given the formulations.

3.10.2. Effect in the nitrosative stress

After 8 weeks of alloxan injection, the sciatic nerve's neural nitrite concentrations of the diabetic control group rats considerably rose, reaching 305.12 ± 3.13 μg/mL ($P < 0.05$), as opposed to the normal control group rats, where a value of 107.17 ± 2.62 μg/mL ($P < 0.05$), was reported. While the values in the treated groups III and IV were

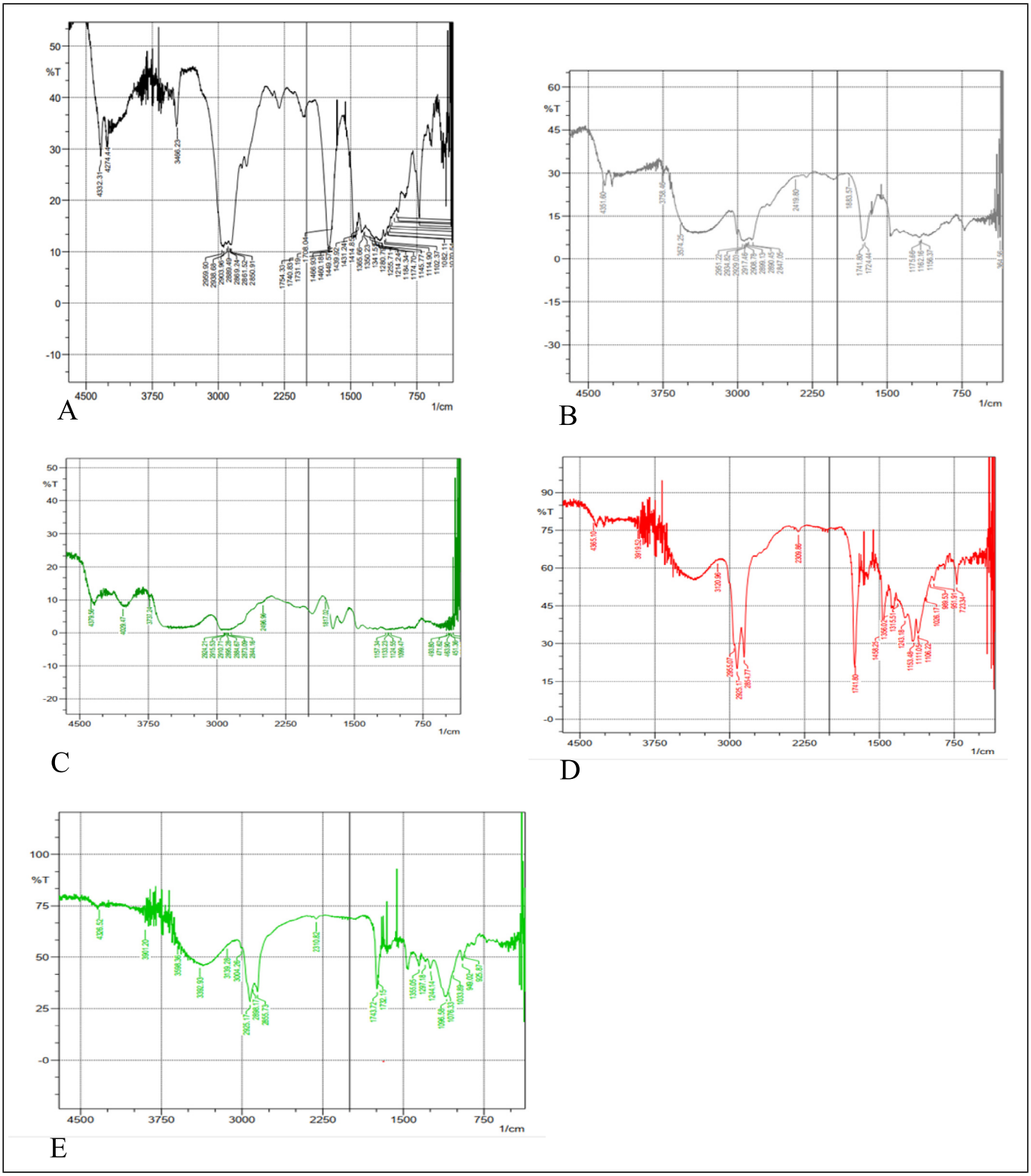

Fig. 11. FTIR Spectra of A: Edible oil; B: Span 80; C:Tween 20; D:F2 and E: F3.

159.10 ± 4.50 and 130.23 ± 5.12, respectively, which are suggestively lower than those in the diabetic control group Table 16.

3.10.3. Effect in lipid peroxide profile

After eight weeks of treatment, LPO levels were found in all groups. In comparison to the normal group, diabetic control groups had significantly higher lipid peroxide profile levels (9.12 ± 1.26 n M/mg of protein). In comparison to the diabetic control group, levels of the treated groups were potentially lowered, measuring 4.20 ± 1.31 nM/mg and 2.90 ± 1.25 nM/mg of protein, in F2 and F3, respectively (Table 16).

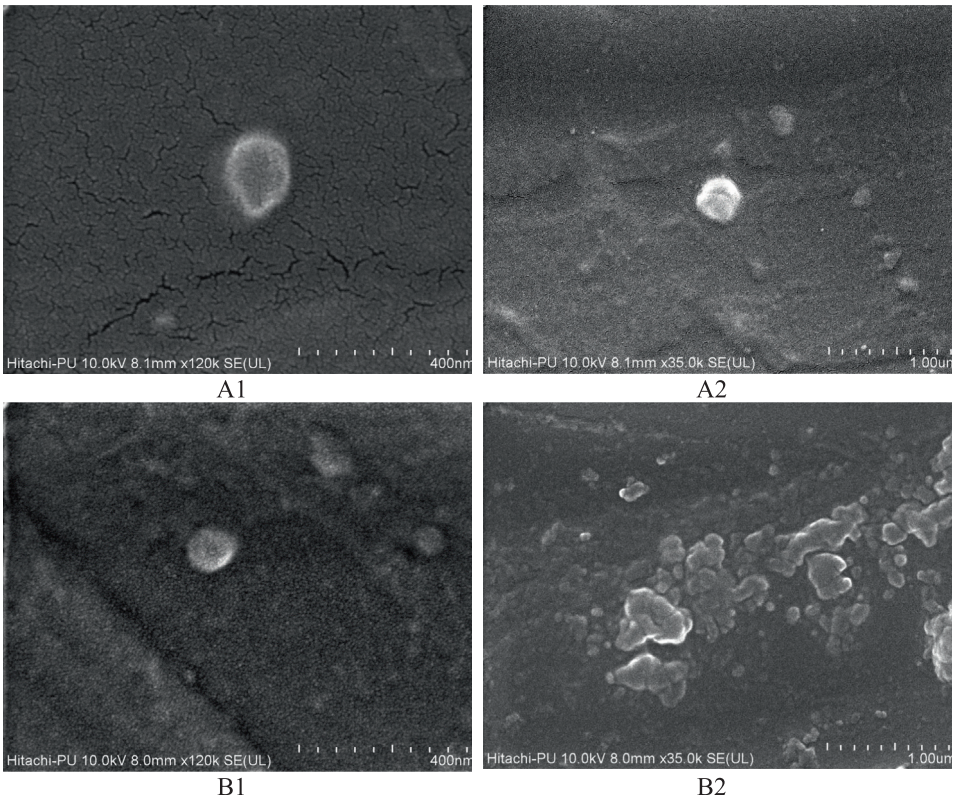

Fig. 12. FESEM image of Formulations. FESEM image of O/W Nanoemulsion F2 and F3 in A and B respectively: (A1) and (B1) image observed under scale of 400 nm and (A2) and (B2) image observed under scale (1 μm).

3.10.4. Effect in membrane-bound inorganic phosphate

After eight weeks of experimental study the level of Na^+K^+-ATPase, is much lower in comparison to the normal control group, was determined to be 2.76 ± 1.25 μmol/mg of protein in the diabetic control group. Values in the treated groups were noticeably higher than in the diabetic control groups. Groups F2 and F3 had values of 7.12 ± 4.20 μmol/mg and 9.40 ± 2.52 μmol/mg of protein, respectively (Table 16).

3.10.5. Effect in the TNF-α

TNF-α levels in the sciatic nerves of diabetic control groups increased significantly from 53.47 ± 2.14 μg/mL to 160.12 ± 2.32 μg/mL, respectively, compared to the control group. In comparison to the diabetic group, Groups III and IV's levels (90.18 ± 1.39 μg/mL and 68.43 ± 1.72 μg/mL, respectively) significantly decreased Table 16.

3.11. Histopathology

Histopathology of organ of rats were done and observed under microscope for the changes as shown in Fig. 14, Fig. 15, Fig. 16 and Fig. 17.

During the study of kidney in the diabetic control group shows an inappropriate structure of the nephron cell with the existence of high endocytic vacuoles and F2 treated group shows partially recovered nephron cells whereas F3 treated group rats shows recovered appropriate structure of the nephron cells with typical glomeruli. Also, metformin-treated standard group shows recovered normal arrangement (Fig. 14).

Diring the study of liver, diabetes management enhanced vacuolation in the cytoplasm of hepatocytes in rat liver and is evident as fuzzy clear vacuoles, which is a sign of glycogen infiltration in diabetes. Liver of the rat treated with F2 exhibits normal architecture with hepatocytes arranged in normal sheets or cord around the central vein; and F3 shows improved liver function in diabetic rats (Fig. 15).

During the stduty it was found the control group of rats, showing numerous focal necrosis of gastric mucosa, whereas F2 treated rat shows a appropriate histological arrrangement of gastric layers, and F3 treated rats show normal epithelial tissue, alongwith metformin treated standard group showing normal gastric mucosa and submucosa (Fig. 16).

During the study of Sciatic nerve, the diabetic control group displayed abnormal nerve fibres and substantial axonal edoema. In the F2 treated group, there was modest localised peripheral axonal loss and lipoid axon degeneration. A decreased axonal degeneration in F3 group lacking regenerative characteristics. Standard metformin-treated diabetic animals showed the normal arrangement of nerve fibres (Fig. 17).

4. Discussion

Diabetes is a long-term condition of the metabolism of carbohydrates, fats, and proteins marked by elevated fasting and post-meal blood glucose levels. According to estimates, the incidence of diabetes will rise from 4% in 1995 to 5.4% by 2025. The WHO predicts that developed nations will bear the brunt of the burden. According to research conducted in India over the past ten years, diabetes is not only more common than it should be but is also spreading quickly among urban residents. In India, there are thought to be 33 million persons who have diabetes. By 2025, this figure is probably going to rise to 57.2 million (Kc et al., 2015, Choudhury et al., 2018). The consequences of the disease account for a large portion of the burden of diabetes mellitus on both individuals and society. As the morbidity and mortality rate in diabetic patients increases with complications, it has now become the need to study it

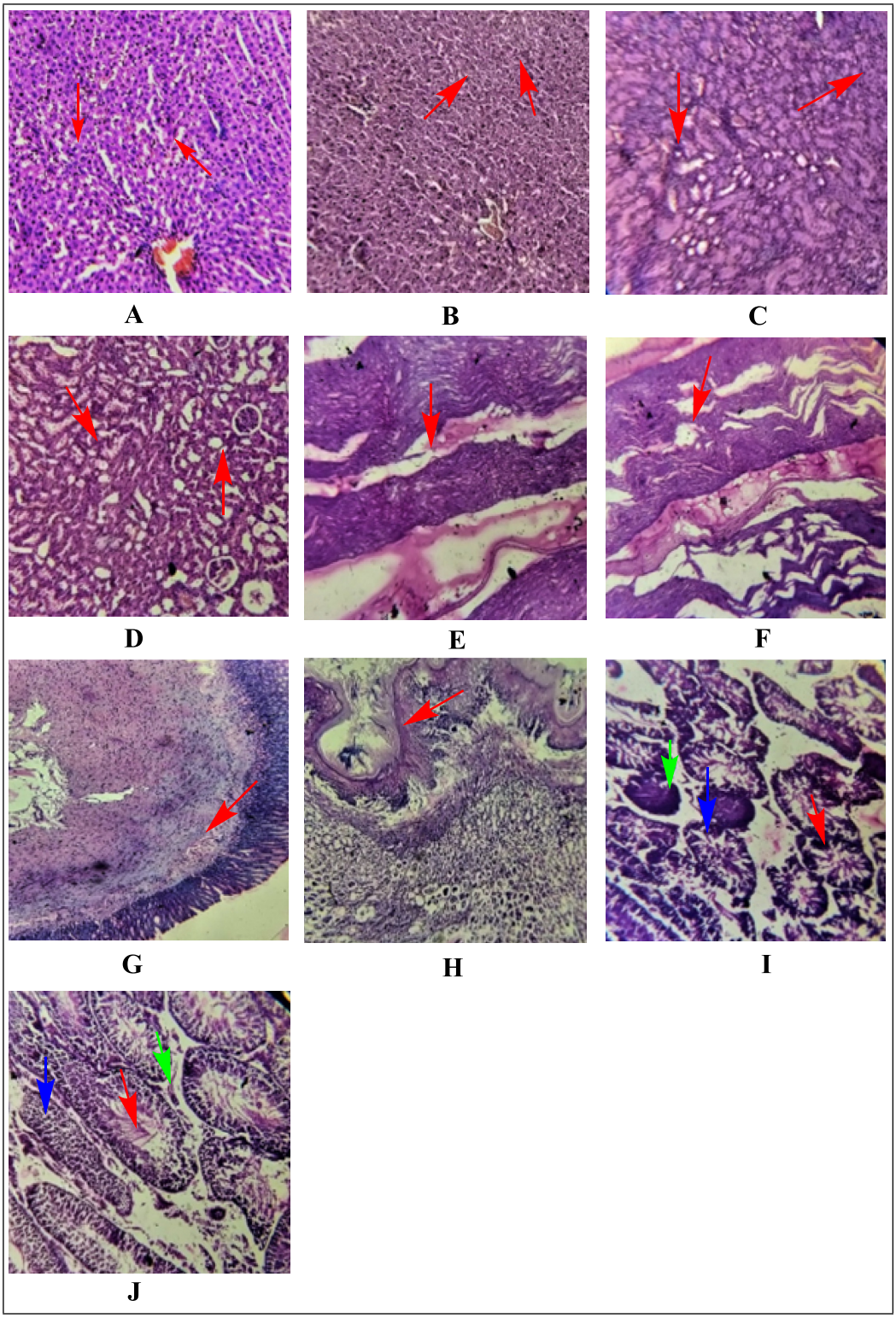

Fig. 13. Histopathology of rat's organs during acute oral toxicity studies (100X). For formaulation F2: A, C, E, G, I and formulation F3: B, D, F, H, J. (A) liver demonstrating normal hepatocytes (arrow); (B) liver showing normal hepatocytes (arrow); (C) The renal tissue shows fairly well-preserved renal parenchyma. The renal tubules around renal corpuscles appeared apparently normal. Inflammatory changes in the renal parenchyma are not evident; (D) The renal tissue shows well preserved renal parenchyma. The renal tubules around renal corpuscles appeared apparently normal. Inflammatory changes in the renal parenchyma are not evident; (E) Showed the normal arrangement of fibers; (F) Showed the normal arrangement of fibers; (G) Normal histological structure of gastric layers, arrows show mucosa; (H) Appropriate histological assembly of gastric layers, arrows demonstrate mucosa; (I) Appropriate testicular histology. The active seminiferous tubules (red arrow) and interstitial spaces (green arrow). The seminiferous epithelium (blue arrow) showing active spermatogenesis; (J) Normal testicular histology. The activated seminiferous tubules (red arrow) and interstitial spaces (green arrow). The seminiferous epithelium (blue arrow) demonstrating active spermatogenesis.

Table 8
Effect of formulations on acute oral toxicity in rats.

Parameters	F2	F3
Eyes	NV	NV
Fur	NV	NV
Skin	NV	NV
Mucous membrane	NV	NV
Salivation	NV	NV
Lacrimation	NV	NV
Perspiration	NV	NV
Piloerection	NV	NV
Urinary	NV	NV
Incontinence	NV	NV
Defecation	NV	NV

NV: No Variations.

extensively. Treatment for diabetes and its consequences costs more than $100 billion annually (Zhuo et al., 2013).

Diabetes can cause nephropathy and cognitive impairment. It will adversely affect the overall quality of life of the diabetic person both socially and economically, equal importance is given to their management (Edwards et al., 2008, Cobos-Palacios et al., 2020). According to the literature review, the traditional medications used to treat diabetic neuropathy and nephropathy are linked to a number of negative effects. Herbal medications display various distinct differences when compared to well-defined synthetic treatments, including being reasonably safe and having less side effects in chronic conditions (Bansal et al., 2006).

The most frequent long-term consequence of diabetes that appears to have significant rates of morbidity and mortality is diabetic neuropathy. It causes more hospitalizations than any other diabetic complication and is responsible for 50–75% of non-traumatic amputations (Kaur et al., 2011). There are currently no accepted medicines to maintain the chronic prognosis of peripheral nerve injury, nor has the pharmacological treatment of neuropathic pain been discovered. The prevalence of diabetic neuropathy is close to 10%, even when insulin therapy is used (Kandhare et al., 2012). Literature reports that various plants consisting of antioxidant phytochemicals increase free radical scavenging activities and may prove beneficial for the treatment of diabetic complications (Dureshahwar et al., 2017). As previously said, herbal treatment is believed to be less toxic than current allopathic drugs, with few or no side effects (Gupta et al., 2017). It has been observed from the literature that, *Morus alba* is an effective herb for multiple medicinal properties due to medicinally important chemicals such as Prenylated flavonoid: kuwanon G Diels–Alder-type adducts: mulberrofuran G; albanol B, chrysin found in the bark. It is very economical, naturally available and can be easily consumed, all these properties make it the best drug for Diabetes Mellitus. The flavonoid chrysin present in the stem bark of *Morus alba* is effective in treating Diabetes mellitus.

Table 9
Hematological study for acute oral toxicity study.

Test Name	F2	F3
COMPLETE BLOOD COUNT (CBC)		
Haemoglobin (Spectrophotometry) (g/dL)	14.9 ± 0.35	15 ± 0.36
PCV (Packed Cell Volume) (Analogical Integration) (%)	46.8 ± 0.20	47.17 ± 0.20
Total Leucocyte Count (TLC)(Electrical Impendence) (thou/mm3)	3.9 ± 0.26	4.23 ± 0.22
RBC Count (Electrical Impedance) (mill/mm3)	7.9 ± 0.20	8.27 ± 0.38
MCV (Calculated) (fL)	59 ± 1.82	59.63 ± 1.26
MCH (Calculated) (pg)	32.2 ± 0.20	19 ± 0.42
MCHC (Calculated) (g/dL)	32.2 ± 0.20	31.90 ± 0.40
RDW (%)	14.7 ± 0.79	15.40 ± 0.49
Platelet Count (Electrical Impedance) (thou/mm3)	758.7 ± 13.68	858.67 ± 13.68
Mean Platelet Volume (Calculated) (fL)	23 ± 1.53	25.33 ± 2.33
Differential Leucocyte Count (DLC)		
Neutrophils (%)	23.5 ± 0.95	24.13 ± 1.17
Lymphocytes (%)	69.4 ± 0.38	69.37 ± 0.59
Monocytes (%)	2.5 ± 029	2.50 ± 0.26
Eosinophils (%)	4.1 ± 0.21	3.33 ± 0.56
Basophils (%)	0.6 ± 0.09	0.53 ± 0.12
Absolute Leucocyte Count		
Neutrophils (Calculated) (thou/mm3)	0.4 ± 0.04	0.40 ± 0.04
Lymphocytes (Calculated) (thou/mm3)	4.6 ± 0.20	4.73 ± 0.09
Monocytes (Calculated) (thou/mm3)	0.03 ± 0.003	0.03 ± 0.003
Eosinophils (Calculated) (thou/mm3)	0.05 ± 0.01	0.06 ± 0.003

Table 10
Observation of rats during pharmacological study.

Parameters	Normal Control	Diabetic Control	Treated Group- F2	Treated Group- F3	Standard
Eyes	NV	SR	SR	NV	NV
Fur	NV	SY	SY	NV	NV
Skin	NV	NV	NV	NV	NV
Mucous membrane	NV	IF	NV	NV	NV
Salivation	NV	DC	SD	SD	SD
Lacrimation	NV	DC	SD	SD	SD
Perspiration	NV	IN	SI	SI	SI
Piloerection	NV	NV	NV	NV	NV
Urinary	NV	IN	SI	SI	SI
Incontinence	NV	IN	SI	SI	SI
Defecation	NV	IN	SI	SI	SI

NV: No Variations; SR: Slightly Red; SY: Slightly Yellow; IF: Inflammation; IN: Increased, SI: Slightly Increased; DC: Decreased; SD: Slightly Decreased.

Table 11
Body weight observation of rats.

Week	Normal Control	Diabetic Control	F2 Treated	F3 Treated	Standard
Zero	265.2 ± 4.38	262.2 ± 3.96	266 ± 4.55	265 ± 4.44	263.8 ± 4.16
Two	273.8 ± 4.81	256.7 ± 3.75[a]	260.7 ± 4.51	262.2 ± 4.48	262.5 ± 4.19
Four	280 ± 4.18	250.8 ± 3.22[a]	256 ± 4.43	257 ± 4.28	258.5 ± 4.21
Six	288.2 ± 2.17	246.8 ± 3.12[a]	251 ± 3.02	252 ± 3.12	253.7 ± 3.62*
Eight	297.3 ± 2.44	239.2 ± 2.55[a]	246.7 ± 3.42*	247.7 ± 3.18***	250.7 ± 3.12***

Values are demonstrated as Mean ± SEM; n = 6. One-way ANOVA; followed by Dunnett's test: [a]P < 0.05 in comparison with normal control; *P < 0.05 and ***P < 0.001 in comparison with the diabetic control.

Table 12
Evaluation of F2 and F3 against Tail-immersion (hot water/heat-allodynia) test.

Groups	2nd week	4th week	8th week
Normal control	14.30 ± 0.56	14.70 ± 0.33	14.30 ± 0.56
Diabetic Control	9.00 ± 0.37[a]	9.70 ± 0.42[a]	9.30 ± 0.67[a]
F2	12.30 ± 0.42**	12.20 ± 0.48*	15.00 ± 0.37***
F3	12.70 ± 0.49**	13.50 ± 0.50**	14.80 ± 0.31**
Standard	18.00 ± 0.52***	18.50 ± 0.43***	18.70 ± 0.49***

Values are expressed as Mean ± SEM; n = 6. One-way ANOVA; followed by Dunnett's test: [a]P < 0.05 in comparison with normal control; *P < 0.05, **P < 0.01 and ***P < 0.001 in comparison with the diabetic control.

Table 13
Evaluation of F2 and F3 against Hot-plate (heat-allodynia) test.

Groups	2nd week	4th week	8th week
Normal control	13.80 ± 0.48	14.20 ± 0.31	14.80 ± 0.31
Diabetic Control	9.00 ± 0.52[a]	9.70 ± 0.56[a]	8.80 ± 0.60[a]
F2	13.20 ± 0.48**	12.70 ± 0.42*	14.70 ± 0.49**
F3	13.00 ± 0.58**	13.70 ± 0.42**	14.20 ± 0.70**
Standard	16.50 ± 0.43***	17.00 ± 0.73***	17.00 ± 0.73***

Values are expressed as Mean ± SEM; n = 6. One-way ANOVA; followed by Dunnett's test: [a]P < 0.05 in comparison with normal control; *P < 0.05, **P < 0.01 and ***P < 0.001 in comparison with the diabetic control.

Table 14
Evaluation of F2 and F3 against Rotarod test.

Groups	2nd week	4th week	8th week
Normal control	39.3 ± 1.28	40.0 ± 1.00	39.0 ± 0.45
Diabetic Control	29.0 ± 0.58[a]	30.8 ± 1.08[a]	31.0 ± 1.06[a]
F2	32.8 ± 1.08*	34.3 ± 1.26**	34.5 ± 0.76**
F3	33.8 ± 1.56**	33.8 ± 2.12**	34.5 ± 0.76**
Standard	35.2 ± 1.56***	38.3 ± 2.49***	39.0 ± 2.74***

Values are expressed as Mean ± SEM; n = 6. One-way ANOVA; followed by Dunnett's test: [a]P < 0.05 in comparison with normal control; *P < 0.05, **P < 0.01 and ***P < 0.001 in comparison with the diabetic control.

Table 15
Evaluation of F2 and F3 against Actophotometer test.

Groups	2nd week	4th week	8th week
Normal control	50.0 ± 1.06	50.3 ± 0.67	51.0 ± 0.63
Diabetic Control	44.8 ± 1.19[a]	46.2 ± 1.01[a]	46.8 ± 0.70[a]
F2	50.2 ± 1.05**	51.2 ± 1.01*	52.5 ± 1.12*
F3	50.3 ± 1.17**	51.5 ± 0.85**	53.0 ± 1.18**
Standard	49.8 ± 0.95**	51.2 ± 1.01*	52.0 ± 1.00*

Values are expressed as Mean ± SEM; n = 6. One-way ANOVA; followed by Dunnett's test: [a]P < 0.05 in comparison with normal control; *P < 0.05, **P < 0.01 and ***P < 0.001 in comparison with the diabetic control.

4.1. Diabetic neuropathy experimental animal model: Alloxan model

Alloxan-induced diabetic rats were used as a reliable model and recurrent hyperglycemic disorders were used to imitate neuropathy features to study the effect of plant extract on neuropathy. As previously said, diabetogenic alloxan dosage serves as a beta-cell toxin, causing beta-cell death and eventually insulin deficiency, culminating in hyperglycemia. Alloxan causes an uptick in reactive oxygen species (ROS), which causes DNA damage and is a key factor in beta-cell death. The multiple-dose induction procedure causes programmed and permanent loss of beta-cells, resulting in chronic diabetes in the experimental model. When persistent hyperglycemia was generated and diabetic neuropathy advanced, the research design was chosen, and treatments were initiated. Clinical manifestations of peripheral diabetic neuropathy include elevated vibration and temperature perception thresholds that result in sensory loss, along with deterioration of fibre types in the peripheral nerve (Bansal et al., 2006). Diabetic neuropathy is clinically characterised by allodynia, hyperalgesia brought on by an enhanced neuronal hypoxia, nociceptive response, and a lower threshold for painful stimuli (Jensen and Finnerup 2014, Rosenberger et al., 2020). An alloxan-induced diabetic model, the most widely used animal model of painful diabetic neuropathy, has similar symptoms (Zychowska et al., 2013).

4.2. Extraction and phytochemical investigation

Extraction of stem bark was done using ethanol. Then phytochemical screening was done to evaluate the presence of different phytoconstituents which was shown in Table 1. As flavonoids were present so for isolating chrysin column chromatography was done. In which solvent n-hexane: ethyl acetate (3:7), gave the isolated compound chrysin. Further, the characterization of chrysin was done by NMR, IR and MASS spectroscopy (Rauf et al., 2015).

4.3. Development of formulation and safety assessment

After isolation and characterization of chrysin, 4 Nanoemulsion formulation was made by using different ratios of ingredients. Then characterization of the formulation was done by evaluating its viscosity, Refractive index, pH, stability, zeta potential, FTIR and FESEM. In stability testing formulation 1 and formulation 4 showed phase separation. Keeping the surface tension lowest to wet the surface to enhance the penetration.on the basis of these two parameters F1 and F4 were discarded. F2 and F3 were further taken for animal experimental work (Rauf et al., 2015). This may be due to adsorbed layers of polymers/large molecules shifting the plane of shear to a farther distance from the particle surface. This leads to a reduction of the measured zeta potential. That means a relatively low ZP will be measured even in the case of highly charged particle surfaces. Despite the low ZP, the formulations are stable (Quaglia et al., 2009).

Safety studies are used to assess a drug's short-term side effects whether given in a single dose or several doses over 24 h. The safety studies were carried out on F2 and F3. Different doses of 2000 mg/kg were injected into rats, and the results showed no evidence of any toxicity within the acceptable range specified by

Table 16
Effect of F2 and F3 on endogenous biomarkers in rats.

Treatment Type	Endogenous Biomarker				
	SOD (µ/mg of Protein)	NO (µg/mL)	LPO (nM/mg of protein)	Na^+K^+ATPase (µmol/mg of protein)	TNF-α (µg/mL)
NC	26.13 ± 1.75	107.17 ± 2.62	2.58 ± 1.29	10.12 ± 1.46	53.47 ± 2.14
DC	5.51 ± 1.34[a]	305.12 ± 1.13[a]	9.12 ± 1.26[a]	2.76 ± 1.25[a]	160.12 ± 2.32[a]
F2	20.35 ± 1.34*	159.10 ± 1.50*	4.20 ± 1.31*	7.12 ± 1.20*	90.18 ± 1.39*
F3	24.28 ± 1.42*	130.23 ± 1.12*	2.90 ± 1.25*	9.40 ± 2.52*	68.43 ± 1.72*
Standard	15.14 ± 1.32*	226.34 ± 2.35***	6.25 ± 1.11*	6.37 ± 1.25*	119.21 ± 1.14*

Values are expressed as Mean ± SEM; n = 6. One-way ANOVA; followed by Dunnett's test: [a]P < 0.05 in comparison with normal control; *P < 0.05, **P < 0.01 and ***P < 0.001 in comparison with the diabetic control.

OECD No. 423 recommendations. No mortality was also observed (OECD 2002).

4.4. Behavioral assessment of diabetic neuropathy and its mechanism

In the current study, rats who received Alloxan injections had considerably higher glucose levels, which triggered diabetic neuropathy and neuropathic pain. Different behavioural parameters were used to assess the neuropathy of rats such as heat allodynia, locomotor activity and motor coordination. Due to an initial burst from the injured peripheral nerve and subsequent prolonged activation of peripheral nociceptors, the dorsal horn neurons in the spinal cord become centrally sensitive after a peripheral nerve injury. The emergence of long-lasting thermal allodynia and hyperalgesia, often referred to as tail heat-allodynia, is significantly influenced by this central sensitization. During the tail-immersion (hot water/heat-allodynia) test, F2 shows statistically significant (P < 0.001) increase in latency in 8th week of the analysis. Also the standard drug increases the latency significantly (P < 0.001) in 4th and 8th week. The normal control group had no sensitivity, the diabetic control group showed higher sensitivity towards pain, treated groups F2 and F3 showed less sensitivity and the standard group showed the lowest sensitivity towards pain as evident in the hot-plate (heat-allodynia) test. Simialar type of study were carried out by the group of scientist (Saraswat et al., 2020a, 2020b).

In comparison to the diabetes control groups, the treated groups showed significant improvements in grip strength, locomotor responses recorded by rotarod and actophotometer. As a result of the fact that diabetic animals eventually develop lethargic responses and inflammation in their nerves, which causes pain in their limbs, the animals' locomotor responses are delayed, and they have a tendency to become less active as their diabetes worsens and diabetic neuropathy takes shape (AlSharari et al., 2014). As from the data of our results it is found that F2 and F3 showed significant increase in responses. Histopathological evaluation shows that disruption caused by alloxon in various organs were controlled by the ingesting the F2 and F3.

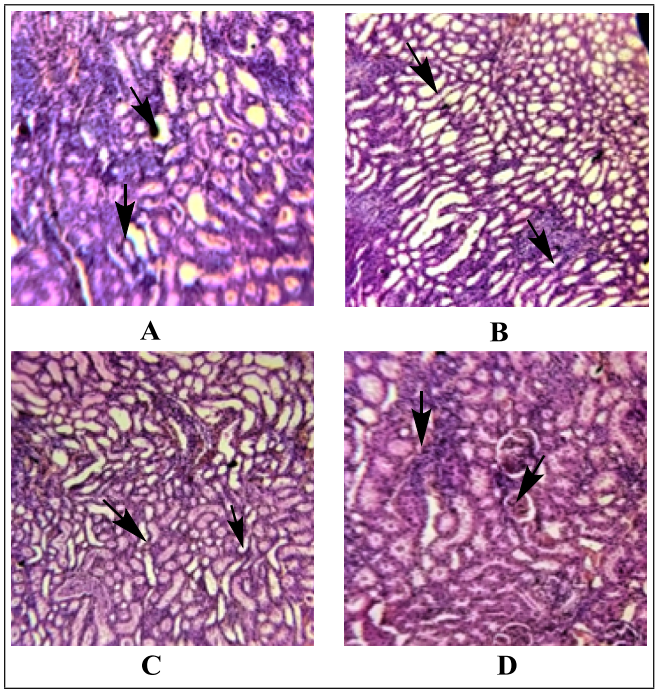

Fig. 14. Histopathology of kidney of rats (100X). (A) The arrow in the diabetic control group shows an inappropriate structure of the nephron cell with the existence of high endocytic vacuoles; (B) the arrow in the F2 treated group shows partially recovered nephron cells; (C) the arrow in the F3 treated group rats shows recovered appropriate structure of the nephron cells with typical glomeruli; and (D) the arrow in the metformin-treated standard group shows recovered normal arrangement.

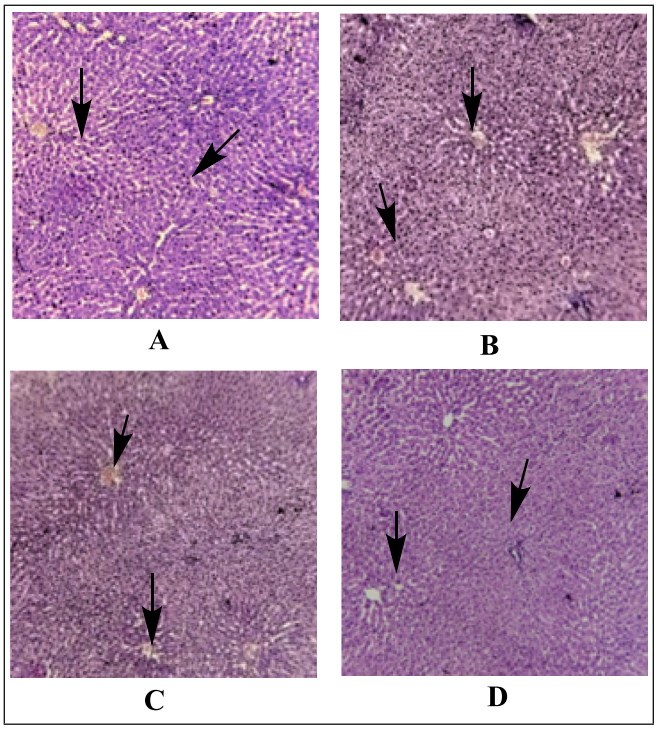

Fig. 15. Histopathology of liver of rats (100X). (A) diabetes management Enhanced vacuolation in the cytoplasm of hepatocytes in rat liver is evident as fuzzy clear vacuoles (arrows), which is a sign of glycogen infiltration in diabete; (B) the liver of the rat treated with F2 exhibits normal liver architecture with hepatocytes arranged in normal sheets or cord around the central vein; and (C) F3 shows improved liver function in diabetic rats (arrow).

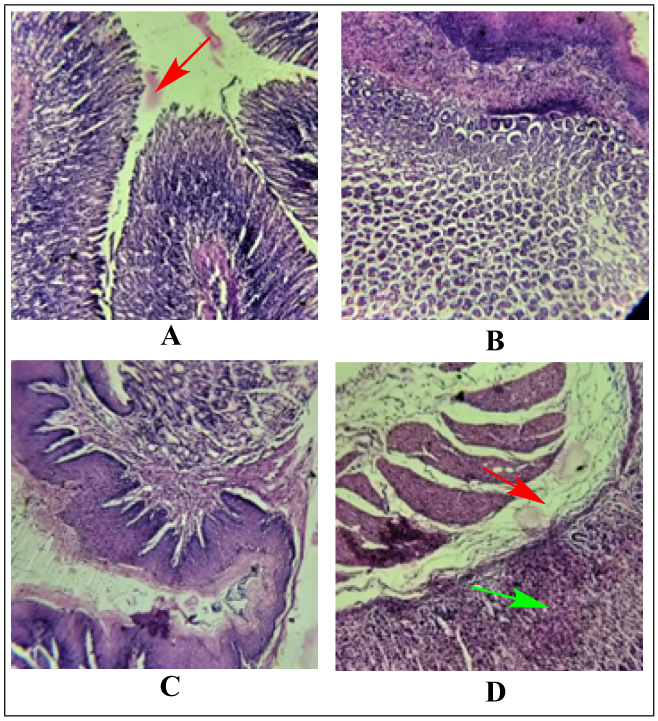

Fig. 16. Histopathology of stomach of rats (100X). (A) Control group rats, showing numerous focal necrosis of gastric mucosa (arrow), (B) F2 treated rat shows a appropriate histological arrrangement of gastric layers, (C) F3 treated rat shows normal epithelial tissue, (D) Metformin treated standard group showing normal gastric mucosa (Red arrow) and submucosa (Green arrow).

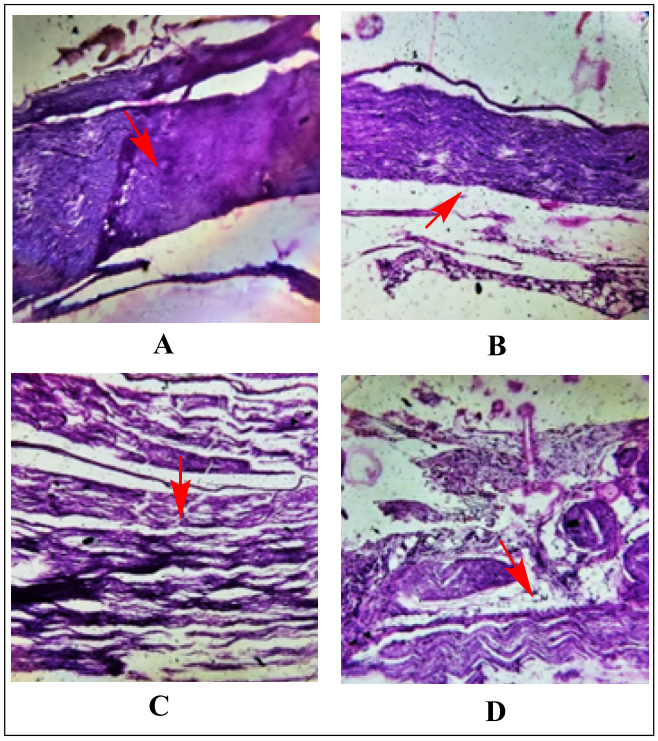

Fig. 17. Histopathology sciatic nerve of rats (100X). (A) Those in the diabetic control group displayed abnormal nerve fibres and substantial axonal edoema; (B) In the F2 group, there was modest localised peripheral axonal loss and lipoid axon degeneration (C) decreased axonal degeneration in F3 group lacking regenerative characteristic (D) Standard metformin-treated diabetic animals showing the normal arrangement of nerve fibres.

SOD and MDA, two endogenous enzymes, are directly associated to oxidative stress. Endothelial damage is caused by endogenous enzymes and superoxide. Protein kinase C and aldose reductase activity rise as a result of the superoxide anions, and these changes are associated to the sense of pain. SOD converts superoxide anions into H_2O_2 to act as an antioxidant defense against them. By reorganizing the bonds in the unsaturated fatty acids of the membrane and contributing significantly to the breakdown of lipid membranes, MDA represents the high stress conditions and damages tissue. Increased lipid peroxidation serves as an indicator of oxidative stress, and pharmacological therapy lowers its levels. Nitric oxide, an intracellular messenger, plays a crucial part in many disease processes. Reactive oxygen species, which function as an antioxidant, react with it. This oxidation is general and has an impact on cell molecules (Cotter and Cameron 2003). When superoxide anions and NO combine, peroxynitrite is formed, which raises NO levels and causes DNA impairment, rapid nitrosylation, LPO, and cell death. In the end, this results in aggravation and increased discomfort. Tetrakis-2-Fe (III) (N-triethylene glycol monomethyl ether) The catalyst for peroxynitrite disintegration that interrelates with diabetic groups' sensory neuropathy is pyridyl porphyrin. The findings of F2 and F3 groups of rats statistically significant ($P < 0.05$) and are consistent with earlier research that was done (Islam et al., 2015).

The synthesis and transmission of bioelectricity are connected to the Na^+K^+ATPase enzyme's uniform distribution. Chronic hyperglycemia conditions resulted in decreased activity of Na^+K^+ATPase enzyme, which inactivates phosphate. The polyol pathways are also activated as a result of it. Na^+K^+ATPase is thereby blocked, and their restoration is favoured. In the recent investigation, F2 and F3 have increased Na^+K^+ATPase levels, demonstrating their neuroprotective effects (Rivelli et al., 2012).

The acceleration of TNF-α production in microvascular and neural tissues is a defining trait of diabetic neuropathy, which results in nerve injury and micro-vascular permeability microangiopathy. For the treatment of diabetic neuropathy problems, the use of drugs that suppress the cytokine increase is indicated. As a result, F2 and F3 reduces TNF-α demonstrates how it contributes to the control of the increased cytokines (Tiwari et al., 2011).

This study also showed a clear correlation between the onset of diabetic neuropathy in diabetic rats and the prominent injury shown in these animals during an eight-week period. A significant contributory factor to the emergence of hyperglycemia and neuropathy in diabetes is an increase in inflammatory levels (Brownlee et al., 1988). The inflammatory indicators are overexpressed in people with diabetes, which leads to cell death and malfunction. In diabetic control group animals, the sciatic nerve displayed infiltration and inflammation, whereas the treated groups displayed healthy tissues (Djordjevic et al., 2015).

In many cultures around the world, using therapeutic plants as a foundation to treat different illness conditions is a prevalent practice. The majority of people still use herbal home remedies, traditional medications, and ayurvedic treatments (extracts, ghritas, and churnas) to treat illness (Saraswat et al., 2020a, 2020b).

The effects of the chrysin-derived formulation on behaviour, histopathology, and biochemistry have been demonstrated in the current investigation. The usual medication has reduced glucose levels, but it is less successful at reducing biomarkers; as a result, it is less beneficial than a formulation derived from chrysin in treating diabetic neuropathy. However, by modulating the release of inflammatory cytokines, TNF-α, oxidative stress, which is a key mediator of apoptotic conditions, neuropathic pain, and restoration of Na^+K^+ATPase activity, the F2 and F3 have both reduced the diabetic condition's severity and restored the neuropathic pain. Chrysin dramatically reduced the pain associated with diabetic neuropathy by involving mechanisms that resulted in the

inhibition of increased cytokines, the restoration of Na^+K^+ATPase levels, a drop in NO levels, and a reduction in TNF-α demonstrating the herb's isolated chrysin's anti-oxidant and therapeutic properties.

5. Conclusion

An attempt has been made to evaluate isolated phytoconstituent derived formulation from the bark of *Morus alba* against alloxan-induced diabetic neuropathy in rats followed by designing a novel drug delivery system. It can be concluded that isolated flavonoid (chrysin) from ethanolic extract of bark of *Morus alba*. has protective and beneficial effects on diabetic neuropathy. Furthermore, a novel drug delivery system called Nanoemulsion was successfully prepared and evaluated to show beneficial action in diabetic neuropathy and mechanism behind it was justified. Thus, this phytoconstituent (chrysin) and Nanoemulsion have a future scope for being used in the treatment of diabetic neuropathy.

Declaration of Competing Interest

The authors declare that they have no known competing financial interests or personal relationships that could have appeared to influence the work reported in this paper.

Acknowledgement

The authors extend their appreciation to Princess Nourah bint Abdulrahman University Researchers Supporting Project number (PNURSP2023R342), Princess Nourah bint Abdulrahman University, Riyadh, Saudi Arabia for supporting this research.

The authors also extend their appreciation to the Researchers Supporting Project number (RSPD2023R628), King Saud University, Riyadh, Saudi Arabia for supporting this research.

Authors contributions

All authors contributed equally towards the project design, execution and write up.

References

Ali, H.H., Hussein, A.A., 2017. Oral nanoemulsions of candesartan cilexetil: formulation, characterization and in vitro drug release studies. AAPS Open. 3, 4. https://doi.org/10.1186/s41120-017-0016-7.

AlSharari, S.D., Al-Rejaie, S.S., Abuohashish, H.M., et al., 2014. Ameliorative potential of morin in streptozotocin-induced neuropathic pain in rats. Trop. J. Pharm. Res. 13. https://doi.org/10.4314/tjpr.v13i9.8.

Arabshahi-Delouee, S., Urooj, A., 2007. Antioxidant properties of various solvent extracts of mulberry (Morus indica L.) leaves. Food Chem. 102, 1233–1240. https://doi.org/10.1016/j.foodchem.2006.07.013.

Baboota, S., Shakeel, F., Ahuja, A., et al., 2007. Design, development and evaluation of novel nanoemulsion formulations for transdermal potential of celecoxib. Acta Pharm. (Zagreb, Croatia) 57, 315–332. https://doi.org/10.2478/v10007-007-0025-5.

Banda, M., Nyirenda, J., Muzandu, K., et al., 2018. Antihyperglycemic and antihyperlipidemic effects of aqueous extracts of lannea edulis in alloxan-induced diabetic rats. Front. Pharmacol. 9, 1099. https://doi.org/10.3389/fphar.2018.01099.

Bansal, V., Kalita, J., Misra, U.K., 2006. Diabetic neuropathy. Postgrad. Med. J. 82, 95–100. https://doi.org/10.1136/pgmj.2005.036137.

Batiha, G.-E.-S., Al-Snafi, A.E., Thuwaini, M.M., et al., 2023. Morus alba: a comprehensive phytochemical and pharmacological review. Naunyn Schmiedebergs Arch. Pharmacol. 396, 1399–1413. https://doi.org/10.1007/s00210-023-02434-4.

Baxi, H., Habib, A., Hussain, M.S., et al., 2020. Prevalence of peripheral neuropathy and associated pain in patients with diabetes mellitus: Evidence from a cross-sectional study. J. Diabetes Metab. Disord. 19, 1011–1017. https://doi.org/10.1007/s40200-020-00597-y.

Bogner, A., Jouneau, P.H., Thollet, G., et al., 2007. A history of scanning electron microscopy developments: towards "wet-STEM" imaging. Micron (Oxford, England : 1993) 38, 390–401. https://doi.org/10.1016/j.micron.2006.06.008.

Bonting, S.J., 1970. Sodium-potassium activated adenosine triphosphatase and cation transport. Membrane Ion Transport.

Brodusch, N., H. Demers and R. Gauvin, 2018. Introduction. Field Emission Scanning Electron Microscopy: New Perspectives for Materials Characterization. N. Brodusch, H. Demers and R. Gauvin. Singapore, Springer Singapore, pp. 1-4.

Brownlee, M., Cerami, A., Vlassara, H., 1988. Advanced glycosylation end products in tissue and the biochemical basis of diabetic complications. N. Engl. J. Med. 318, 1315–1321. https://doi.org/10.1056/nejm198805193182007.

Callaghan, B.C., Little, A.A., Feldman, E.L., et al., 2012. Enhanced glucose control for preventing and treating diabetic neuropathy. The Cochrane database of systematic reviews. CD007543. https://doi.org/10.1002/14651858.CD007543.pub2.

Choudhury, H., Pandey, M., Hua, C.K., et al., 2018. An update on natural compounds in the remedy of diabetes mellitus: a systematic review. J Tradit Complement Med. 8, 361–376. https://doi.org/10.1016/j.jtcme.2017.08.012.

Cobos-Palacios, L., Sampalo, A.L., Carmona, M.D.L., 2020. Neuropatía diabética. Medicine - Programa de Formación Médica Continuada Acreditado. 13, 911–923. https://doi.org/10.1016/j.med.2020.09.013.

Cotter, M.A., Cameron, N.E., 2003. Effect of the NAD(P)H oxidase inhibitor, apocynin, on peripheral nerve perfusion and function in diabetic rats. Life Sci. 73, 1813–1824. https://doi.org/10.1016/s0024-3205(03)00508-3.

Deacon, R.M., 2013. Measuring motor coordination in mice. J Vis Exp. e2609. https://doi.org/10.3791/2609.

Djordjevic, A., Bursac, B., Velickovic, N., et al., 2015. The impact of different fructose loads on insulin sensitivity, inflammation, and PSA-NCAM-mediated plasticity in the hippocampus of fructose-fed male rats. Nutr Neurosci. 18, 66–75. https://doi.org/10.1179/1476830513Y.0000000098.

Dordevic, S.M., Santrac, A., Cekic, N.D., et al., 2017. Parenteral nanoemulsions of risperidone for enhanced brain delivery in acute psychosis: physicochemical and in vivo performances. Int. J. Pharm. 533, 421–430. https://doi.org/10.1016/j.ijpharm.2017.05.051.

Dureshahwar, K., Mubashir, M., Une, H.D., 2017. Quantification of Quercetin Obtained from Allium cepa Lam. Leaves and its effects on streptozotocin-induced diabetic neuropathy. Pharmacognosy Res. 9, 287–293. https://doi.org/10.4103/pr.pr_147_16.

Eddy, N.B., Touchberry, C.F., Lieberman, J.E., 1950. Synthetic analgesics; methadone isomers and derivatives. J. Pharmacol. Exp. Ther. 98, 121–137.

Edwards, J.L., Vincent, A.M., Cheng, H.T., et al., 2008. Diabetic neuropathy: mechanisms to management. Pharmacol. Ther. 120, 1–34. https://doi.org/10.1016/j.pharmthera.2008.05.005.

Ercisli, S., Orhan, E., 2007. Chemical composition of white (Morus alba), red (Morus rubra) and black (Morus nigra) mulberry fruits. Food Chem. 103, 1380–1384. https://doi.org/10.1016/j.foodchem.2006.10.054.

Grover, M., Makkar, R., Sehgal, A., et al., 2020. Etiological aspects for the occurrence of diabetic neuropathy and the suggested measures. Neurophysiology 52, 159–168. https://doi.org/10.1007/s11062-020-09865-2.

Gupta, R.C., Chang, D., Nammi, S., et al., 2017. Interactions between antidiabetic drugs and herbs: an overview of mechanisms of action and clinical implications. Diabetol Metab Syndr. 9, 59. https://doi.org/10.1186/s13098-017-0254-9.

Gupta, R.B., Kompella, U.B., 2006. Nanoparticle technology for drug delivery. Taylor & Francis Group LLc..

Islam, B.U., Habib, S., Ahmad, P., et al., 2015. Pathophysiological role of peroxynitrite induced DNA damage in human diseases: a special focus on Poly(ADP-ribose) Polymerase (PARP). Indian J. Clin. Biochem. : IJCB. 30, 368–385. https://doi.org/10.1007/s12291-014-0475-8.

Jensen, T.S., Finnerup, N.B., 2014. Allodynia and hyperalgesia in neuropathic pain: clinical manifestations and mechanisms. Lancet Neurol. 13, 924–935. https://doi.org/10.1016/s1474-4422(14)70102-4.

Kanaan, S.A., Saade, N.E., Haddad, J.J., et al., 1996. Endotoxin-induced local inflammation and hyperalgesia in rats and mice: a new model for inflammatory pain. Pain 66, 373–379. https://doi.org/10.1016/0304-3959(96)03068-0.

Kandhare, A.D., Raygude, K.S., Ghosh, P., et al., 2012. Neuroprotective effect of naringin by modulation of endogenous biomarkers in streptozotocin induced painful diabetic neuropathy. Fitoterapia 83, 650–659. https://doi.org/10.1016/j.fitote.2012.01.010.

Kaur, S., Pandhi, P., Dutta, P., 2011. Painful diabetic neuropathy: an update. Ann Neurosci. 18, 168–175. https://doi.org/10.5214/ans.0972-7531.1118409.

Kc, K., Shakya, S., Zhang, H., 2015. Gestational diabetes mellitus and macrosomia: a literature review. Ann. Nutr. Metab. 66 (Suppl 2), 14–20. https://doi.org/10.1159/000371628.

Kulkarni, S.K., 2005. Handbook of Experimental Pharmacology. Delhi, Vallabh Prakashan.

Kumkoon, T., Srisaisap, M., Boonserm, P., 2023. Biosynthesized silver nanoparticles using Morus alba (White Mulberry) leaf extract as potential antibacterial and anticancer agents. Molecules (Basel, Switzerland). 28. https://doi.org/10.3390/molecules28031213.

Liang, C.-X., Qi, D.-L., Zhang, L.-N., et al., 2021. Preparation and evaluation of a water-in-oil nanoemulsion drug delivery system loaded with salidroside. Chin. J. Nat. Med. 19, 231–240. https://doi.org/10.1016/s1875-5364(21)60025-0.

Morrow, T.J., 2004. Animal models of painful diabetic neuropathy: the STZ rat model. Current protocols in neuroscience, Unit 9.18 (Chapter 9). https://doi.org/10.1002/0471142301.ns0918s29.

Nagani, K., Kaneria, M., Chanda, S., 2012. Pharmacognostic studies on the leaves of Manilkara zapota L. (Sapotaceae). Pharmacognosy J. 4, 38–41. https://doi.org/10.5530/pj.2012.27.6.

Necker, R., Hellon, R.F., 1978. Noxious thermal input from the rat tail: modulation by descending inhibitory influences. Pain 4, 231–242. https://doi.org/10.1016/0304-3959(77)90135-x.

OECD, 2002. Test No. 423: Acute Oral toxicity - Acute Toxic Class Method.

Onyambu, M., Gikonyo, N., Nyambaka, H., et al., 2020. Macroscopic and microscopic features of diagnostic value for Warburgia ugandensis Sprague leaf and stem-bark herbal materials. J. Pharmacogn. Phytother. 12, 36–43. https://doi.org/10.5897/JPP2019.0569.

Pathak, R., Sachan, N., Chandra, P., 2022. Mechanistic approach towards diabetic neuropathy screening techniques and future challenges: a review. Biomed. Pharmacother. = Biomedecine & pharmacotherapie. 150,. https://doi.org/10.1016/j.biopha.2022.113025 113025.

Quaglia, F., Ostacolo, L., Mazzaglia, A., et al., 2009. The intracellular effects of non-ionic amphiphilic cyclodextrin nanoparticles in the delivery of anticancer drugs. Biomaterials 30, 374–382. https://doi.org/10.1016/j.biomaterials.2008.09.035.

Rauf, A., Khan, R., Raza, M., et al., 2015. Suppression of inflammatory response by chrysin, a flavone isolated from Potentilla evestita Th. Wolf. In silico predictive study on its mechanistic effect. Fitoterapia 103, 129–135. https://doi.org/10.1016/j.fitote.2015.03.019.

Razavi, R., Molaei, R., Moradi, M., et al., 2019. Biosynthesis of metallic nanoparticles using mulberry fruit (Morus alba L.) extract for the preparation of antimicrobial nanocellulose film. Appl. Nanosci. 10, 465–476. https://doi.org/10.1007/s13204-019-01137-8.

Rivelli, J.F., Amaiden, M.R., Monesterolo, N.E., et al., 2012. High glucose levels induce inhibition of Na, K-ATPase via stimulation of aldose reductase, formation of microtubules and formation of an acetylated tubulin/Na, K-ATPase complex. Int. J. Biochem. Cell Biol. 44, 1203–1213. https://doi.org/10.1016/j.biocel.2012.04.011.

Rosenberger, D.C., Blechschmidt, V., Timmerman, H., et al., 2020. Challenges of neuropathic pain: focus on diabetic neuropathy. J. Neural Transm (Vienna). 127, 589–624. https://doi.org/10.1007/s00702-020-02145-7.

Saraswat, N., Sachan, N., Chandra, P., 2020a. Anti-diabetic, diabetic neuropathy protective action and mechanism of action involving oxidative pathway of chlorogenic acid isolated from Selinum vaginatum roots in rats. Heliyon. 6, e05137.

Saraswat, N., Sachan, N., Chandra, P., 2020b. A review on ethnobotanical, phytochemical, pharmacological and traditional aspects of indigenous Indian herb Trachyspermum ammi (L). J. Curr. Traditional Med. 6, 172–187.

Slaoui, M., Fiette, L., 2011. Histopathology procedures: from tissue sampling to histopathological evaluation. Methods Mol. Biol. (Clifton N.J.) 691, 69–82. https://doi.org/10.1007/978-1-60761-849-2_4.

Sofowora, A., 1996. Research on medicinal plants and traditional medicine in Africa. J. Alternative Complementary Med. 2, 365–372.

Sriraksa, N., Kongsui, R., Thongrong, S., et al., 2019. Effect of Azadirachta indica flower extract on functional recovery of sciatic nerve crush injury in rat models of DM. Exp. Ther. Med. 17, 541–550. https://doi.org/10.3892/etm.2018.6931.

Srivastava, S., Kapoor, R., Thathola, A., et al., 2006. Nutritional quality of leaves of some genotypes of mulberry (Morus alba). Int. J. Food Sci. Nutr. 57, 305–313. https://doi.org/10.1080/09637480600801837.

Ting, P., Srinuanchai, W., Suttisansanee, U., et al., 2021. Development of chrysin loaded oil-in-water nanoemulsion for improving bioaccessibility. Foods. 10. https://doi.org/10.3390/foods10081912.

Tiwari, V., Kuhad, A., Chopra, K., 2011. Emblica officinalis corrects functional, biochemical and molecular deficits in experimental diabetic neuropathy by targeting the oxido-nitrosative stress mediated inflammatory cascade. Phytother. Res. : PTR. 25, 1527–1536. https://doi.org/10.1002/ptr.3440.

Trease, G.E., Evans, W.C., 1983. Pharmacognosy. Saunders Company, Philadelphia, W.B.

Valcheva-Kuzmanova, S., Georgieva, A., Belcheva, I., et al., 2015. Anxiolytic-Like Effect of Chlorogenic Acid Administered Subchronically to Rats. C. R. Acad. Bulg. Sci. 68, 1463+.

Yadav, P.S., Yadav, E., Verma, A., et al., 2014. Development, characterization, and pharmacodynamic evaluation of hydrochlorothiazide loaded self-nanoemulsifying drug delivery systems. Sci. World J. 2014,. https://doi.org/10.1155/2014/274823 274823.

Ye, F., Shen, Z., Xie, M., 2002. Alpha-glucosidase inhibition from a Chinese medical herb (Ramulus mori) in normal and diabetic rats and mice. Phytomed.: Int. J. Phytother. Phytopharmacol. 9, 161–166. https://doi.org/10.1078/0944-7113-00065.

Zhang, R., Zhang, Q., Zhu, S., et al., 2022. Mulberry leaf (Morus alba L.): A review of its potential influences in mechanisms of action on metabolic diseases. Pharmacol. Res. 175,. https://doi.org/10.1016/j.phrs.2021.106029 106029.

Zhuo, X., Zhang, P., Hoerger, T.J., 2013. Lifetime direct medical costs of treating type 2 diabetes and diabetic complications. Am. J. Prev. Med. 45, 253–261. https://doi.org/10.1016/j.amepre.2013.04.017.

Zychowska, M., Rojewska, E., Przewlocka, B., et al., 2013. Mechanisms and pharmacology of diabetic neuropathy – experimental and clinical studies. Pharmacol. Rep. 65, 1601–1610. https://doi.org/10.1016/s1734-1140(13)71521-4.